drug; however, it is practically difficult to directly compare all classes of antihypertensive agents at the same time in a single intervention trial. This cross-sectional observation therefore aimed to tentatively characterize all classes of antihypertensive agents commonly used in Japan in terms of CBP.

METHODS

Study design. This study was a cross-sectional observation, designed as an exploratory (or data-mining) study to generate rather than to test hypotheses.

Subjects. We enrolled 1,727 Japanese patients with essential hypertension (HT), who had been on stable antihypertensive medication for at least 3 months, and with medical data, including radial artery tonometry-derived parameters relating to CBP, from seven major centers and their related medical facilities participating in the Antihypertensives and Blood pressure of Central artery study in Japan (ABC-J). The subjects also included 1,094 participants receiving no antihypertensive therapy. From the untreated population, 848 nonhypertensive (non-HT) subjects were extracted based on BP (systolic BP (SBP) <140 mm Hg and diastolic BP (DBP) <90 mm Hg) measured when the radial artery pulse wave was recorded (Table 1).

The study protocol was approved by the institutional review board of each ABC-J center. Data were obtained from archived medical records of participants in whom the radial artery pulse wave had been recorded in accordance with the method described below. All participants were informed of this study procedure and gave consent to providing their data. The data were collected from January to December in 2007.

Radial artery pulse wave measurement and evaluation of CBP. Radial artery pressure pulse waveform was recorded with an automated tonometric system, HEM-9000AI (Omron Healthcare, Kyoto, Japan) in a sitting position after at least 5 min of rest. The waveform was calibrated automatically using built-in oscillometric brachial sphygmomanometry. The peak and bottom of the radial pressure wave were adjusted to brachial SBP and DBP, respectively. The HEM-9000AI algorithm automatically performed online detection of the second peak (late systolic inflection) based on the second maxima of the fourth derivative of the radial pressure waveform to determine the radial augmentation index as well as the late or second SBP (SBP2), as shown in Figure 1. The outline of the built-in algorithm of this device has been reported elsewhere.[15]

In order to assess CBP-lowering effects selectively, we focused on central SBP levels relative to brachial SBP because absolute CBP levels largely depend on the mean BP level, which is nearly identical for both central and peripheral sites.[16] Figure 1 shows the parameters derived from radial pulse waveform analysis. The height of the second peak corresponds to SBP2, which is reportedly an alternative[17] to or is closely related[18] to directly measured central aortic SBP. SBP2 obtained by the same device as in this study has also been reported to be comparable to central SBP estimated using a generalized aorto-radial transfer function.[19,20] We created an index, ΔSBP2, defined as "SBP2 − SBP" (Figure 1), to assess peak SBP reduction between peripheral and central sites.

Therapeutic drugs. Antihypertensive drugs being administered at the time of measurement were obtained from medical records together with coadministered antidyslipidemia and antidiabetic drugs, nitrates and/or nicorandil. All class names and antihypertensive abbreviations are in the footnote of Table 2.

Data analysis. All data are expressed as the mean ± 1 s.d. unless otherwise specified. Intergroup comparisons of mean values and ratios of subjects' characteristics were tested by unpaired Student's *t*-test and Fisher's exact test, respectively. Multiple regression analysis (forced entry method) was employed to compare all classes of, as well as broadly grouped (vasodilating (VD) and non-VD), antihypertensive drugs in terms of the association with ΔSBP2, where VD included angiotensin receptor blockers (ARB), ACEI, CCB, and α-blocker; and non-VD included Diur and βBL. Categorical data, such as gender and drugs, were assessed as dummy variables ("0" or "1") in regression models. For VD and non-VD, we made a dummy variable, "Drug group," which was coded "1" if the patient took any one or several non-VD drugs without VD drugs in combination whereas code "0" indicated any others, including any one or several VD drugs and mixed combinations of VD plus non-VD drugs. In Model 1 in Table 3, where patients with mixed combination were excluded from the subject population, code "0" implied that a patient took

Table 1 | Subject characteristics

	Treated HT	Non-HT	*P*
N (pts)	1,727	848	
Male/female (pts)	884/843	468/380	0.059
Age (years)	66.5 ± 11.5	50.3 ± 16.7	<0.001
Height (cm)	157.6 ± 9.3	162.4 ± 9.6	<0.001
Weight (kg)	60.0 ± 11.4	59.2 ± 10.5	0.109
BMI (kg/m^2)	24.0 ± 3.4	22.4 ± 2.9	<0.001
PR (bpm)	69.2 ± 12.0	69.1 ± 10.4	0.949
Calibrated radial artery tonometry			
SBP (mm Hg)	137.7 ± 17.2	118.4 ± 11.6	<0.001
SBP2 (mm Hg)	127.6 ± 18.3	106.7 ± 14.3	<0.001
DBP (mm Hg)	74.8 ± 11.8	70.0 ± 8.9	<0.001
rAI (%)	85.5 ± 14.0	76.7 ± 17.1	<0.001
Number of drugs in combination, pts (%)			
1	596 (34.5%)		
2	632 (36.6%)		
3	390 (22.6%)		
4	97 (5.6%)		
5	12 (0.7%)		

BMI, body mass index; BP, blood pressure; DBP, diastolic blood pressure; Diur, diuretics; HT, treated hypertensives; non-HT, nonhypertensives; PR, pulse rate; pts, number of patients; rAI, radial augmentation index; SBP, systolic blood pressure; SBP2, late systolic blood pressure.

any one or several VD drugs only. Multiple regression models were used for adjusted comparisons of individual classes or broadly divided groups of antihypertensive drugs and their combinations, in which determinants of ΔSBP2 other than a specified antihypertensive drug or a drug combination were adjusted. Because pulse rate is largely attributable to the drug effect itself, it was not adjusted unless otherwise specified. The adjusted comparisons were as follows:

1. A multiple regression model was constructed for ΔSBP2 forcing all possible independent variables, including all antihypertensive drugs either broadly grouped (VD vs. non-VD) or grouped by drug class, to enter the models. Interactive terms relating to drug combinations were examined and significant interactive terms were considered to be included in the model.
2. For the non-HT population, a separate model without the drug variable was constructed. Based on this model, ΔSBP2 was modified by adjusting common confounders (age, gender, height, BMI, DBP) to the mean value of HT. This provided the estimated physiological reference value of ΔSBP2 when the DBP level was comparable with treated HT.
3. We collected adjusted ΔSBP2 data for an individual group or class of antihypertensive agents by extracting cases given a specified type of drugs irrespective of monotherapy or combination. Likewise, data for each combination of two specified antihypertensive classes were collected, including combinations of ≥3 drugs.
4. In addition to adjusting for all common confounders and the use of nitrates (="0"), further adjustments of ΔSBP2 were made for each specified group or class of drugs or their combination. For interdrug group or interclass comparisons, variables for irrelevant classes coadministered and interactive terms were set as "0" (i.e., not used). Similarly, for intercombination therapy comparisons, variables for coadministered drugs not included in the specified combination as well as interactive terms (unless applicable) were set as "0."
5. Interdrug group, interclass or intercombination therapy comparisons of CBP indexed by ΔSBP2 were made using the adjusted data, as described above. Adjusted ΔSBP2 was also compared between each drug group and non-HT. Two-group comparisons, including VD only vs. non-VD only and each drug group vs. non-HT, were tested by the Mann–Whitney U-test, whereas interclass and intercombination therapy as well as intertreatment group (i.e., VD vs. non-VD vs. Mixed) comparisons were tested by the Kruskal–Wallis test with multiple comparisons by the Games–Howell method.

All statistical analyses were performed with a commercially available statistical package (SPSS, version 11.0; SPSS, Chicago, IL) and spreadsheet calculation (Excel 2007; Microsoft, Washington, DC). *P* values <0.05 were regarded as significant.

RESULTS

Subjects' characteristics and details of antihypertensive therapy are shown in **Tables 1** and **2**. Overall, ≥60% patients were treated with CCB or ARB. Only one third of participants was treated with monotherapy (**Table 1**), and monotherapy with some classes of drugs was very rare (**Table 2**), which made it difficult to compare all individual antihypertensive classes directly. We therefore first examined broadly divided drug groups, i.e., VD and non-VD. As shown in **Table 3**, partial regression coefficient (*B*) estimates of "Drug group" in Models 1 and 2 consistently indicated that ΔSBP2 was 2.7 mm Hg higher with non-VD than with VD when all included confounders were adjusted.

In 510 participants who provided a detailed clinical data set, including laboratory data and comorbidities, none showed significant associations with ΔSBP2 by multiple regression

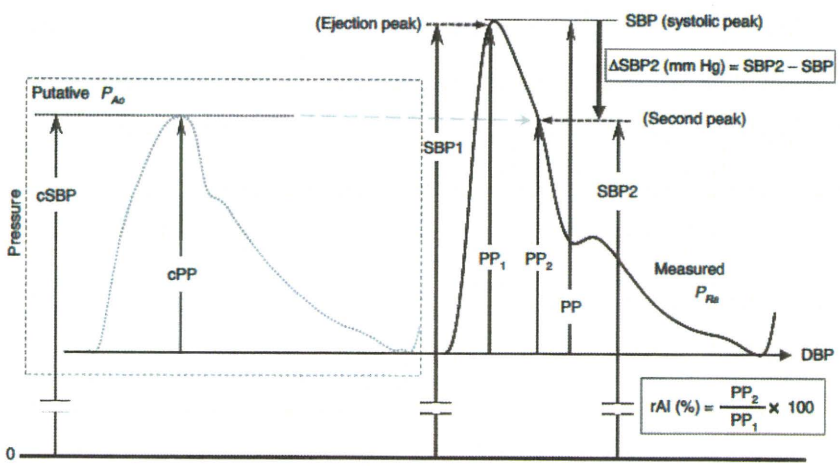

Figure 1 | Definitions of ΔSBP2 and radial augmentation index (rAI), and relationship between each parameter derived from calibrated tonometric radial pressure waveform (P_{Ra} = solid line; right) and corresponding putative aortic pressure waveform (P_{Ao} = dotted line; left). These definitions are expressed as formulas inside the Figure. cPP, central pulse pressure; cSBP, central systolic blood pressure; DBP, diastolic blood pressure; PP, radial pulse pressure; PP_1, ejection peak amplitude of P_{Ra}; PP_2, second peak amplitude of P_{Ra}; SBP, radial peak systolic blood pressure; SBP1, radial artery pressure at the ejection peak, which is not necessarily identical to the systolic peak of P_{Ra}; SBP2, radial artery pressure at the second peak.

Table 2 | Details of antihypertensive therapy

	Class of antihypertensives[a]						
	ARB	ACEI	CCB	αBL	Diur	βBL	Nitro
N (pts (%))	1,019 (59.0)	207 (12.0)	1,178 (68.2)	161 (9.3)	422 (24.4)	373 (21.6)	121 (7.0)
Male/female (pts)	537/482	125/82	601/577	87/74	190/232	189/184	84/37
Age (years)	66.7±11.7	64.8±13.2	67.4±10.7	65.7±10.9	66.6±11.4	66.5±11.0	73.3±8.2
Height (cm)	157.7±9.5	158.7±9.7	157.1±9.3	157.7±8.0	157.0±9.4	158.4±9.0	157.5±8.4
Weight (kg)	60.6±11.8	60.3±11.5	60.1±11.5	61.9±11.2	61.7±11.6	61.5±11.4	57.8±9.2
BMI (kg/m^2)	24.2±3.5	23.8±3.2	24.2±3.4	24.8±3.7	25.0±3.6	24.4±3.5	23.2±2.7
PR (bpm)	69.1±11.8	70.9±13.1	69.1±12.2	68.1±12.9	68.2±12.2	63.7±11.2	69.0±13.0
Calibrated radial artery tonometry							
SBP (mm Hg)	138.5±17.3	137.4±17.1	138.2±16.9	138.9±17.3	134.4±18.1	134.5±17.6	139.2±16.4
SBP2 (mm Hg)	128.1±18.7	126.3±18.1	127.7±18.0	126.8±18.0	124.8±18.1	126.2±18.9	125.3±18.1
DBP (mm Hg)	74.9±12.0	75.0±11.5	74.6±11.6	73.7±12.3	71.7±12.6	73.2±11.8	72.2±10.9
rAI (%)	85.0±13.9	83.8±13.9	85.3±14.0	83.6±15.5	85.5±13.1	88.2±14.5	80.9±14.8
Number of drugs prescribed:							
1 (pts)	235	54	274	0	26	34	16
≥2 (pts)	784	153	904	161	396	339	105
	Drug classes used in combination[b]						
	ARB+CCB	ARB+Diur	ARB+βBL	CCB+ACEI	CCB+Diur	CCB+βBL	Diur+βBL
N (pts (%))	633 (36.7)	274 (15.9)	201 (11.6)	120 (6.9)	267 (15.5)	257 (14.9)	116 (6.7)
Male/female (pts)	345/288	123/151	106/95	72/48	122/145	127/130	54/62
Age (years)	67.7±11.4	67.6±11.0	67.1±11.5	67.2±10.8	67.6±10.7	66.4±11.2	65.9±11.4
Height (cm)	157.4±9.6	156.5±9.5	158.2±9.3	157.5±9.9	156.3±9.1	158.2±9.2	158.2±9.3
Weight (kg)	61.0±12.2	61.7±12.0	62.4±12.4	60.2±11.7	61.4±11.1	62.0±11.3	64.5±11.9
BMI (kg/m^2)	24.5±3.6	25.1±3.7	24.8±3.9	24.1±3.3	25.1±3.6	24.7±3.4	25.7±3.9
PR (bpm)	69.0±12.1	68.2±12.1	63.0±11.0	71.9±13.9	67.4±11.9	63.4±11.1	62.8±10.7
Calibrated radial artery tonometry							
SBP (mm Hg)	139.3±17.1	135.1±18.3	135.6±18.2	140.1±15.3	135.2±17.8	134.8±16.9	130.3±18.7
SBP2 (mm Hg)	128.2±18.7	125.2±18.1	127.1±20.0	128.1±16.0	125.1±17.2	126.1±18.5	122.4±19.4
DBP (mm Hg)	74.2±12.0	71.7±12.4	72.8±12.6	75.4±11.1	72.0±11.8	72.8±11.7	70.8±12.1
rAI (%)	84.6±14.4	85.2±13.1	88.1±14.0	83.6±13.6	85.3±12.4	87.5±14.0	87.5±14.3
Number of drugs prescribed							
2 (pts)	309	66	28	62	40	67	2
≥3 (pts)	324	208	173	58	227	190	114

ACEI, angiotensin-converting enzyme inhibitors; ARB, angiotensin receptor blockers; CCB, calcium channel blockers; DBP, diastolic blood pressure; Diur, diuretics; Nitro, nitrates or nicorandil; pts, number of patients; αBL, α-blockers; βBL, β-blockers.
[a]Because of its vasoactive action, Nitro is included although drugs in this class are not classified as antihypertensives. [b]The number for each specified drug combination includes patients taking three or more antihypertensives other than the specified drugs.

analysis (**Supplementary Table S1a** online). We further examined the multiple regression models individually, including each clinical variable available in this study. Although the total cholesterol level (N = 784; B = 0.02 mm Hg·dl/mg; P = 0.01), serum creatinine (N = 1,374; B = −0.27 mm Hg·dl/mg; P = 0.04), and hemoglobin (N = 868; B = 0.27 mm Hg·dl/g; P = 0.03) reached a significant level, only modest influences on the B estimates of "Drug group" were observed (**Supplementary Table S1b** online).

ΔSBP2 data adjusted using Model 1 were compared between VD only and non-VD only as well as with non-HT, in which adjusted ΔSBP2 was estimated based on Model 3 (area A in Figure 2). Although the difference between VD and non-VD was evident, N with actual non-VD only was far fewer than with VD only, which resulted in larger variance in this group. We then estimated ΔSBP2 with VD only or non-VD only in patients with mixed combination therapy based on Model 2, which increased the number of data compared. The results are shown with adjusted data of actual mixed combination within area B in Figure 2. Estimated ΔSBP2 with VD alone (−10.1 mm Hg) was lower than with non-VD alone (−6.6 mm Hg), and even lower than in non-HT (−7.7 mm Hg).

Table 3 | Multiple regression models of ΔSBP2 in specified populations

	Model 1				Model 2				Model 3			
N	1,094				1,711				848			
Adjust R^2	0.366				0.366				0.553			
Independent variables	***B***	**95% CI**	***β***	***P***	***B***	**95% CI**	***β***	***P***	***B***	**95% CI**	***β***	***P***
Physical variables												
Gender	−2.808	−3.963 to −1.654	−0.170	<0.001	−2.687	−3.571 to −1.803	−0.169	<0.001	−4.539	−5.645 to −3.432	−0.292	<0.001
Age	−0.002	−0.040 to 0.036	−0.003	0.921	−0.005	−0.035 to 0.026	−0.007	0.764	0.176	0.151 to 0.201	0.378	<0.001
Height	−0.186	−0.251 to −0.120	−0.212	<0.001	−0.170	−0.221 to −0.119	−0.199	<0.001	−0.119	−0.181 to −0.057	−0.147	<0.001
BMI	−0.293	−0.410 to −0.175	−0.120	<0.001	−0.210	−0.301 to −0.120	−0.090	<0.001	−0.469	−0.598 to −0.340	−0.174	<0.001
Hemodynamic variables												
PR	−0.342	−0.375 to −0.308	−0.492	<0.001	−0.336	−0.362 to −0.310	−0.508	<0.001	−0.238	−0.273 to −0.203	−0.318	<0.001
DBP	0.149	0.114 to 0.184	0.212	<0.001	0.141	0.114 to 0.168	0.210	<0.001	0.257	0.214 to 0.300	0.295	<0.001
Group of drugs												
Nitro	−3.393	−5.058 to −1.728	−0.098	<0.001	−3.631	−4.913 to −2.350	−0.109	<0.001				
Drug group	2.678	0.984 to 4.372	0.075	0.002	2.709	1.073 to 4.345	0.064	0.001				
Mixed					0.448	−0.209 to 1.105	0.027	0.181				

Drug group: code "1" = treated with non-VD only; code "0" = other treatments with VD only and mixed combination with VD and non-VD. Mixed: code "1" = mixed combination with VD and non-VD; code "0" = all other treatments (with VD only or non-VD only). VD (vasodilating antihypertensive drugs) includes angiotensin receptor blockers, angiotensin-converting enzyme inhibitors, calcium channel blockers, and α-blockers; non-VD (nonvasodilating antihypertensive drugs) includes diuretics and β-blockers. Subject populations for Models 1 through 3 were hypertensives (HT) without mixed (VD + non-VD) combination, HT including mixed combination except Nitro only and non-HT, respectively. Sixteen HT patients taking Nitro alone were excluded from Models 1 and 2. ΔSBP2 is defined in **Figure 1**. 95% CI, 95% confidence interval of *B*; *B*, nonstandardized partial regression coefficient; BMI, body mass index; DBP, diastolic blood pressure; PR, pulse rate; *β*, standardized partial regression coefficient.

In contrast, with non-VD alone, it was even higher than in non-HT.

To enable the characterization of each individual class, we constructed a model including all classes of antihypertensive agents and a significant interactive term as independent variables (**Table 4**). Only "CCB × Diur" was significant among all interactive terms that could have been assessed previously (**Supplementary Table S2a–d** online). Among antihypertensive classes, ARB, CCB, and α-blockers had significant associations with lower ΔSBP2.

Using this model, we performed adjusted interclass comparisons of antihypertensive drugs to characterize each individual class in terms of ΔSBP2 (**Figure 3a**). Treatments with VD antihypertensive classes showed a lower ΔSBP2 than nonvasodilators comparably to VD and non-VD in **Figure 2**. Most importantly, no significant difference in ΔSBP2 was detected among any VD classes. The mean level of ΔSBP2 (−9.7 mm Hg) was 3.3 and 2.0 mm Hg lower than with nonvasodilators and in non-HT. In contrast, with βBL or diuretics, the averaged ΔSBP2 value was 1.3 mm Hg higher than in non-HT. When pulse rate adjustment was added (**Figure 3b**), the higher level of ΔSBP2 associated with βBL was reduced, which abolished the significant difference from ACEI.

Adjusted comparisons of ΔSBP2 among treatments with frequently used combinations of antihypertensives were also performed (**Figure 4**) based on the model (**Table 4**). The combination of two different VD antihypertensive classes, such as CCB plus ARB or ACEI, showed the lowest level of ΔSBP2 (−10.5 mm Hg; **Figure 4a**), which was lower than in any single VD antihypertensive class shown in **Figure 3a**. When the drug combined with ARB or CCB was a diuretic or βBL, the ΔSBP2 value increased in this order. The combination of diuretics and βBL showed the highest ΔSBP2 (−3.9 mm Hg). Additional pulse rate adjustment tended to reduce ΔSBP2 with βBL-including combinations, whereas its influence varied for Diur-including combinations. Differences between the combination of CCB plus ARB or ACEI and that of diuretics plus βBL remained significant even after pulse rate adjustment.

DISCUSSION

In the present study, all individual classes of antihypertensive agents commonly used in Japan and combinations of two different classes were tentatively characterized in terms of central

Table 4 | Multiple regression models of ΔSBP2 in treated hypertensives

N		1,727		
Adjusted R^2		0.379		
Independent variables	*B*	95% C.I.	*β*	*P*
Physical variables				
Gender	−2.358	−3.236 to −1.480	−0.148	<0.001
Age	−0.004	−0.034 to 0.027	−0.005	0.813
Height	−0.185	−0.235 to −0.134	−0.215	<0.001
BMI	−0.200	−0.290 to −0.109	−0.085	<0.001
Hemodynamic variables				
PR	−0.336	−0.362 to −0.310	−0.508	<0.001
DBP	0.140	0.113 to 0.167	0.207	<0.001
Class of drugs				
ARB	−1.012	−1.682 to −0.343	−0.062	0.003
ACEI	−0.516	−1.512 to 0.479	−0.021	0.309
CCB	−0.837	−1.619 to −0.056	−0.049	0.036
αBL	−2.122	−3.158 to −1.087	−0.077	<0.001
Diur	1.890	0.690 to 3.090	0.102	0.002
βBL	0.537	−0.218 to 1.292	0.028	0.163
Nitro	−3.675	−4.882 to −2.468	−0.118	<0.001
Interactive term				
CCB × Diur	−1.953	−3.414 to −0.493	−0.089	0.009

ACEI, angiotensin-converting enzyme inhibitors; ARB, angiotensin receptor blockers; BMI, body mass index; CCB, calcium channel blockers; DBP, diastolic blood pressure; Diur, diuretics; Nitro, nitrates or nicorandil; PR, pulse rate; αBL, α-blockers; βBL, β-blockers.

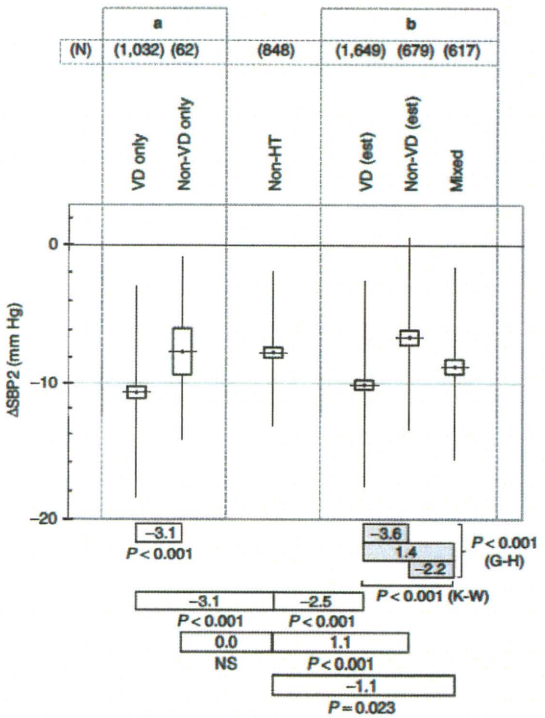

Figure 2 | Adjusted comparisons of ΔSBP2 between vasodilating (VD) and non-VD antihypertensive drugs. VD group includes angiotensin receptor blockers, calcium channel blockers, angiotensin-converting enzyme inhibitors, and α-blockers, and non-VD group includes β-blockers and diuretics. Data are shown as the mean level (horizontal line) and the 95% confidence interval (box height) as well as the range of ±1 s.d. by a vertical error bar. *P* value in the lower part of the figure indicates the result of the Mann–Whitney *U*-test of each specified intergroup comparison unless specified in the figure (K-W, Kruskal–Wallis test; G-H, Games–Howell multiple comparison test). The number in each box indicates the difference (mm Hg) of mean ΔSBP2 between compared groups. Gray area A shows the comparison between actual VD and non-VD only regimens irrespective of the number of drugs. ΔSBP2 data were adjusted for confounding factors (age, gender, height, BMI, DBP, and the use of nitrates = "0") based on Model 1 in **Table 3**. Cases with mixed combination (VD + non-VD) regimens were excluded. Gray area B shows the comparison among VD(est), non-VD(est) and Mixed combinations of VD and non-VD. "(est)" indicates including data derived from mixed combination, for which the effects of VD or non-VD alone on ΔSBP2 were estimated using Model 2 in **Table 3**. Data in the nonhypertensive (non-HT) population indicate the physiological reference value of ΔSBP2 estimated by adjusting confounding factors to the mean value of treated HT using Model 3 in **Table 3**.

effects indexed by ΔSBP2. We found that treatment with any VD antihypertensive class showed lower CBP than any nonvasodilatory class when peripheral BP was lowered to the same level. CBP assessment was highly objective using a validated semiautomatic radial artery tonometry system,[15,19] which could minimize variance and errors related to observer or operator skill.

Feature of ΔSBP2 and its cross-sectional determinants

The augmentation index reportedly depends on age,[21] gender,[22] height,[23] heart rate,[24,25] and BP levels.[26] ΔSBP2 relates to radial augmentation index by definition as radial augmentation index is the ratio of (PP+ΔSBP2) to PP1 (**Figure 1**). The ΔSBP2 value is always negative and reflects the actual reduction in SBP and pulse pressure from peripheral to central sites. Comparing Models 2 and 3 (**Table 3**), significant associations between these variables and ΔSBP2 observed in the non-HT population were partially preserved even in treated HT except for age.

Interpretation of the results

In addition to adjustment for common confounders, model-based estimation of ΔSBP2 compensating for coadministered drug effects enabled interclass comparisons of central effects of antihypertensives that were impossible to make directly with raw data, and played a "data-mining" role in this study.

Central effects of antihypertensive classes. The lower level of CBP, even lower than in non-HT, with VD antihypertensives administered alone (area B in **Figures 2** and **3a**) might lead to more effective unloading of pulsatile mechanical stress on the cardiovascular system than nonvasodilatory agents. The observed reduction of ΔSBP2 with βBL by additional pulse rate adjustment (**Figure 3b**) suggested that the CBP-raising feature of βBL might be attributable to its negative chronotropic effect.

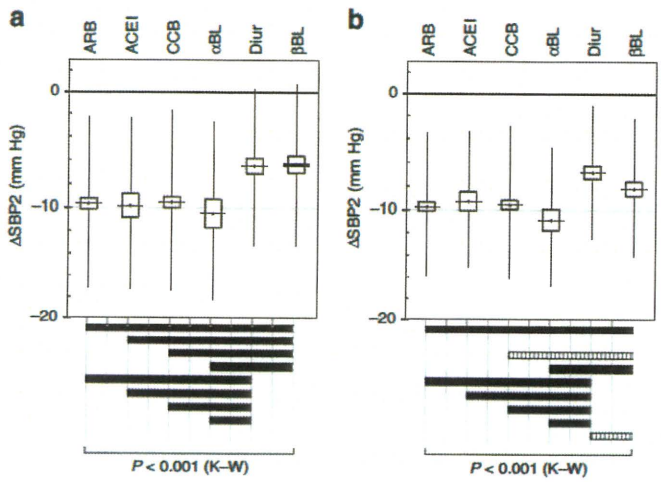

Figure 3 | Adjusted interclass comparisons of ΔSBP2. Data are shown in the same format as in **Figure 2**. A solid or striped horizontal bar in the lower part of the figure denotes a comparison with significant difference determined by Games–Howell multiple comparison test indicating $P < 0.001$ or $P < 0.05$, respectively. The number of patients included in each antihypertensive group is shown in **Table 2** ("Class of antihypertensives"). As indicated in that table, it includes patients treated with two or more drugs in combination as well as patients actually taking the specified drug alone. **(a)** Using the model shown in **Table 4**, ΔSBP2 was adjusted for age, gender, height, BMI, DBP, coadministered drugs (including Nitro = "0") other than the specified antihypertensive class, and the interactive term. **(b)** In addition to the adjustment in **Figure 3a**, ΔSBP2 values were adjusted for pulse rate. ACEI, angiotensin-converting enzyme inhibitors; ARB, angiotensin receptor blockers; CCB, calcium channel blockers; Diur, diuretics; αBL, α-blockers; βBL, β-blockers.

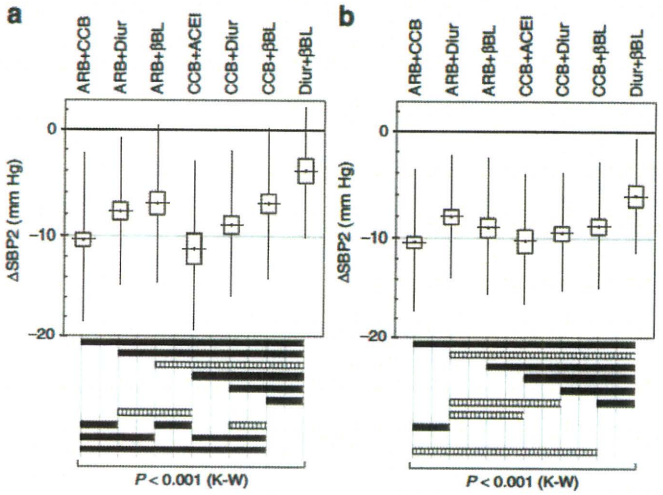

Figure 4 | Adjusted comparisons of ΔSBP2 among frequently used combinations of antihypertensive agents. The number of cases included in each treatment group is indicated in **Table 2** ("Drug classes used in combination"). As indicated in that table, it includes patients treated with three or more drugs as well as patients actually taking only two specified drugs in combination. The format of each graph is as in **Figure 3**. **(a)** Using the model shown in **Table 4**, data were adjusted for age, gender, height, BMI, DBP, and coadministered drugs (including Nitro = "0") other than the specified two-drug combination if applicable. The interactive term was set as "0" except for the CCB+Diur combination. **(b)** In addition to the adjustment in **Figure 4a**, data were also adjusted for pulse rate. ACEI, angiotensin-converting enzyme inhibitors; ARB, angiotensin receptor blockers; CCB, calcium channel blockers; Diur, diuretics; βBL, β- blockers.

Central effects of major combinations of antihypertensive drugs. **Figure 4a** suggested some additive CBP-lowering effects of two different vasodilatory classes. In contrast, along with higher ΔSBP2 above the physiological level with non-VD (**Figure 2**), the findings with non-VD-including combinations suggested that the central effects of non-VD antihypertensives were CBP-raising rather than less potent CBP-lowering.

The negative *B* estimate of the significant interactive term, "CCB × Diur", suggested some synergistic CBP-lowering effect.

Comparison with other studies

The results of this study are consistent with reported studies, such as the CAFE study,[1] and other small-scale studies.[3–11] More recently, other small-scale treatment trials dealing with the effects on CBP of a newer class of antihypertensives, ARB, compared with βBL, have been reported.[27–29] The results of these studies can be summarized as the superiority of vasodilatory antihypertensives, including CCB, ARB, and ACEI, to nonvasodilatory agents, such as diuretics and βBL. Similar to the CAFE study, the higher CBP level with βBL-including treatments was evident in this study; however, these studies used only limited antihypertensive regimens. This cross-sectional observation, including a data-mining model-based estimation process, enabled tentative but simultaneous comparisons of all commonly used antihypertensive agents specifically in terms of central effects by individual class as well as by common combination regimens. Additionally, this study reported ΔSBP2 levels in HT compared with an adjusted physiological reference level.

Limitations

Issues relating to the observational study design. This study was designed as an exploratory study to generate rather than to test hypotheses; therefore, the results cannot confirm the causal effects of each drug class on CBP but provide hypotheses to be assessed. Because of the cross-sectional and observational design, in which the selection of antihypertensive drugs was left to the clinician, and might have been related to patients' clinical characteristics, an indication bias was inevitable. Although we examined available clinical variables in some participants (**Supplementary Tables S1a and S1b** online), they included only some of the population studied and all data could not be adjusted for clinical confounders. The influence of indication bias could therefore not be avoided and should be taken into consideration when interpreting the results of this study.

Issues relating to model-based adjustment. In addition, the results should be interpreted with caution for the following reasons. Data adjustments were based on linear regression models. The influences of adjusted variables are not necessarily linear. Also, the doses and duration of specified antihypertensive medications were not taken into consideration due

to the limited study design. Although the findings obtained from such analysis are not conclusive, we believe that they can provide information to develop hypotheses.

Interpretation of nitrates. As nitrates are not classified as antihypertensive agents, data were compared adjusting for the use of this type of drugs. Only a minority of subjects was given nitrates (Table 2), but significantly lower ΔSBP2 was observed. This may be attributable to, at least in part, cardiac dysfunction,[30,31] because nitrates are usually prescribed for cardiac patients. We could not adjust for cardiac function because of the absence of required information. It is well-known that nitrates markedly reduce aortic wave reflections or late systolic BP augmentation.[4,32,33] In this study, to compare each class of antihypertensives in terms of central effects, the DBP level was adjusted, indicating that the mean pressure-lowering effect was ignored, which was likely to exaggerate the effect of nitrates as a central antihypertensive. Although a small-scale uncontrolled trial using extended-release isosorbide mononitrate has already been reported,[7] randomized intervention trials are necessary to elucidate whether significant associations with lower ΔSBP2 are from pharmacological effects or cardiac dysfunction, as well as its clinical benefit for HT without cardiac dysfunction.

In summary, among all classes of antihypertensive drugs, any single VD antihypertensive agent (CCB, ARB, ACEI, or α-blockers) might lower CBP without interclass difference, whereas nonvasodilators (Diur and βBL) might raise CBP above the physiological level when peripheral BP is adjusted to the same level. The other novel findings obtained in this study are that (i) among assessable combinations, only CCB+Diur showed synergistic interaction; (ii) otherwise, coadministered VD antihypertensives did not affect the CBP-raising features of nonvasodilators; (iii) the CBP-raising effect of βBL is chiefly attributable to negative chronotropism; and (iv) total cholesterol level, serum creatinine, and hemoglobin showed modest but significant associations with ΔSBP2.

Finally, the hypothetical feature of each antihypertensive class in terms of CBP and its prognostic predictive value should be assessed by large-scale randomized intervention trials.

Supplementary material is linked to the online version of the paper at http://www.nature.com/ajh

Acknowledgments: This study was supported by an unrestricted grant from Omron Healthcare. Some of the devices used to measure radial augmentation index and related parameters were rented from Omron Healthcare.

Disclosure: The authors declared no conflict of interest.

1. Williams B, Lacy PS, Thom SM, Cruickshank K, Stanton A, Collier D, Hughes AD, Thurston H, O'Rourke M. Differential impact of blood pressure-lowering drugs on central aortic pressure and clinical outcomes: principal results of the Conduit Artery Function Evaluation (CAFE) study. *Circulation* 2006; 113:1213–1225.
2. Roman MJ, Devereux RB, Kizer JR, Lee ET, Galloway JM, Ali T, Umans JG, Howard BV. Central pressure more strongly relates to vascular disease and outcome than does brachial pressure: the Strong Heart Study. *Hypertension* 2007; 50:197–203.
3. Guerin AP, Pannier BM, Marchais SJ, Metivier F, Safar M, London GM. Effects of antihypertensive agents on carotid pulse contour in humans. *J Hum Hypertens* 1992; 6 Suppl 2:S37–S40.
4. Takazawa K, Tanaka N, Takeda K, Kurosu F, Ibukiyama C. Underestimation of vasodilator effects of nitroglycerin by upper limb blood pressure. *Hypertension* 1995; 26:520–523.
5. Cholley BP, Shroff SG, Sandelski J, Korcarz C, Balasia BA, Jain S, Berger DS, Murphy MB, Marcus RH, Lang RM. Differential effects of chronic oral antihypertensive therapies on systemic arterial circulation and ventricular energetics in African-American patients. *Circulation* 1995; 91:1052–1062.
6. Chen CH, Ting CT, Lin SJ, Hsu TL, Yin FC, Siu CO, Chou P, Wang SP, Chang MS. Different effects of fosinopril and atenolol on wave reflections in hypertensive patients. *Hypertension* 1995; 25:1034–1041.
7. Stokes GS, Ryan M. Can Extended-Release Isosorbide Mononitrate be Used as Adjunctive Therapy for Systolic Hypertension? An Open Study Employing Pulse-Wave Analysis to Determine Effects of Antihypertensive Therapy. *Am J Geriatr Cardiol* 1997; 6:11–19.
8. Pannier BM, Guerin AP, Marchais SJ, London GM. Different aortic reflection wave responses following long-term angiotensin-converting enzyme inhibition and beta-blocker in essential hypertension. *Clin Exp Pharmacol Physiol* 2001; 28:1074–1077.
9. Asmar R, Gosse P, Topouchian J, N'tela G, Dudley A, Shepherd GL. Effects of telmisartan on arterial stiffness in Type 2 diabetes patients with essential hypertension. *J Renin Angiotensin Aldosterone Syst* 2002; 3:176–180.
10. de Luca N, Asmar RG, London GM, O'Rourke MF, Safar ME; REASON Project Investigators. Selective reduction of cardiac mass and central blood pressure on low-dose combination perindopril/indapamide in hypertensive subjects. *J Hypertens* 2004; 22:1623–1630.
11. Morgan T, Lauri J, Bertram D, Anderson A. Effect of different antihypertensive drug classes on central aortic pressure. *Am J Hypertens* 2004; 17:118–123.
12. O'Rourke M. Systolic blood pressure: arterial compliance and early wave reflection, and their modification by antihypertensive therapy. *J Hum Hypertens* 1989; 3 Suppl 1:47–52.
13. O'Rourke MF. Arterial mechanics and wave reflection with antihypertensive therapy. *J Hypertens Suppl* 1992; 10:S43–S49.
14. Ting CT, Chen CH, Chang MS, Yin FC. Short- and long-term effects of antihypertensive drugs on arterial reflections, compliance, and impedance. *Hypertension* 1995; 26:524–530.
15. Melenovsky V, Borlaug BA, Fetics B, Kessler K, Shively L, Kass DA. Estimation of central pressure augmentation using automated radial artery tonometry. *J Hypertens* 2007; 25:1403–1409.
16. Pauca AL, Wallenhaupt SL, Kon ND, Tucker WY. Does radial artery pressure accurately reflect aortic pressure? *Chest* 1992; 102:1193–1198.
17. Pauca AL, Kon ND, O'Rourke MF. The second peak of the radial artery pressure wave represents aortic systolic pressure in hypertensive and elderly patients. *Br J Anaesth* 2004; 92:651–657.
18. Takazawa K, Kobayashi H, Shindo N, Tanaka N, Yamashina A. Relationship between radial and central arterial pulse wave and evaluation of central aortic pressure using the radial arterial pulse wave. *Hypertens Res* 2007; 30:219–228.
19. Richardson CJ, Maki-Petaja KM, McDonnell BJ, Hickson SS, Wilkinson IB, McEniery CM. Comparison of estimates of central systolic blood pressure and peripheral augmentation index obtained from the Omron HEM-9000AI and SphygmoCor systems. *Artery Research* 2009; 3:24–31.
20. Hickson SS, Butlin M, Mir FA, Graggaber J, Cheriyan J, Khan F, Grace AA, Yasmin, Cockcroft JR, Wilkinson IB, McEniery CM; Anglo-Cardiff Collaboration Trial Investigators. The accuracy of central SBP determined from the second systolic peak of the peripheral pressure waveform. *J Hypertens* 2009; 27:1784–1788.
21. Kelly R, Hayward C, Avolio A, O'Rourke M. Noninvasive determination of age-related changes in the human arterial pulse. *Circulation* 1989; 80:1652–1659.
22. Gatzka CD, Kingwell BA, Cameron JD, Berry KL, Liang YL, Dewar EM, Reid CM, Jennings GL, Dart AM. Gender differences in the timing of arterial wave reflection beyond differences in body height. *J Hypertens* 2001; 19:2197–2203.
23. London GM, Guerin AP, Pannier BM, Marchais SJ, Metivier F. Body height as a determinant of carotid pulse contour in humans. *J Hypertens Suppl* 1992; 10:S93–S95.
24. Wilkinson IB, MacCallum H, Flint L, Cockcroft JR, Newby DE, Webb DJ. The influence of heart rate on augmentation index and central arterial pressure in humans. *J Physiol (Lond)* 2000; 525 Pt 1:263–270.
25. Wilkinson IB, Mohammad NH, Tyrrell S, Hall IR, Webb DJ, Paul VE, Levy T, Cockcroft JR. Heart rate dependency of pulse pressure amplification and arterial stiffness. *Am J Hypertens* 2002; 15:24–30.
26. Nürnberger J, Dammer S, Opazo Saez A, Philipp T, Schäfers RF. Diastolic blood pressure is an important determinant of augmentation index and pulse wave velocity in young, healthy males. *J Hum Hypertens* 2003; 17:153–158.

27. Dhakam Z, McEniery CM, Yasmin, Cockcroft JR, Brown MJ, Wilkinson IB. Atenolol and eprosartan: differential effects on central blood pressure and aortic pulse wave velocity. *Am J Hypertens* 2006; 19:214–219.
28. Schneider MP, Delles C, Klingbeil AU, Ludwig M, Kolloch RE, Krekler M, Stumpe KO, Schmieder RE. Effect of angiotensin receptor blockade on central haemodynamics in essential hypertension: results of a randomised trial. *J Renin Angiotensin Aldosterone Syst* 2008; 9:49–56.
29. Vyssoulis GP, Karpanou EA, Kyvelou SM, Adamopoulos DN, Antonakoudis GC, Deligeorgis AD, Cokkinos DV, Stefanadis CI. Beneficial effect of angiotensin II type 1 receptor blocker antihypertensive treatment on arterial stiffness: the role of smoking. *J Clin Hypertens (Greenwich)* 2008; 10:201–207.
30. Westerhof N, O'Rourke MF. Haemodynamic basis for the development of left ventricular failure in systolic hypertension and for its logical therapy. *J Hypertens* 1995; 13:943–952.
31. Nichols WW, O'Rourke MF. *McDonald's Blood Flow in Arteries*, 5th edn. Hodders Arnold: London, 2005.
32. Yaginuma T, Avolio A, O'Rourke M, Nichols W, Morgan JJ, Roy P, Baron D, Branson J, Feneley M. Effect of glyceryl trinitrate on peripheral arteries alters left ventricular hydraulic load in man. *Cardiovasc Res* 1986; 20:153–160.
33. Fitchett DH, Simkus GJ, Beaudry JP, Marpole DG. Reflected pressure waves in the ascending aorta: effect of glyceryl trinitrate. *Cardiovasc Res* 1988; 22: 494–500.

Sympathoinhibition Induced by Centrally Administered Atorvastatin Is Associated With Alteration of NAD(P)H and Mn Superoxide Dismutase Activity in Rostral Ventrolateral Medulla of Stroke-Prone Spontaneously Hypertensive Rats

Takuya Kishi, MD, PhD, Yoshitaka Hirooka, MD, PhD, Satomi Konno, MD, and Kenji Sunagawa, MD, PhD

Abstract: Oxidative stress in the rostral ventrolateral medulla (RVLM) increases sympathetic nervous system activity (SNA). Oral treatment with atorvastatin decreases SNA through antioxidant effects in the RVLM of stroke-prone spontaneously hypertensive rats (SHRSP). We aimed to examine whether centrally administered atorvastain reduces SNA in SHRSP and, if so, to determine whether it is associated with the reduction of oxidative stress induced by alteration of activities of nicotinamide adenine dinucleotide phosphate [NAD(P)H] oxidase and superoxide dismutase (SOD) in the RVLM of SHRSP. SHRSP received atorvastatin (S-ATOR) or vehicle (S-VEH) by continuous intracerebroventricular infusion for 14 days. Mean blood pressure, heart rate, and SNA were significantly lower in S-ATOR than in S-VEH. Oxidative stress, Rac1 activity, NAD(P)H oxidase activity, Rac1, gp91^{phox} and p22^{phox} expression in the membrane fraction, and p47^{phox} and p40^{phox} expression in the cytosolic fraction in the RVLM were significantly lower in S-ATOR than in S-VEH. Rac1 expression in the cytosolic fraction and Mn-SOD activity, however, were significantly higher in S-ATOR than in S-VEH. Our findings suggest that centrally administered atorvastatin decreases SNA and is associated with decreasing NAD(P)H oxidase activity and upregulation of Mn-SOD activity in the RVLM of SHRSP, leading to suppressing oxidative stress.

Key Words: hypertension, sympathetic nerve activity, atorvastatin, oxidative stress, brain

(*J Cardiovasc Pharmacol*™ 2010;55:184–190)

INTRODUCTION

In the brainstem, the rostral ventrolateral medulla (RVLM) is known as one of the vasomotor centers that regulates sympathetic nervous system activity (SNA).[1,2] Previously, we reported that the levels of reactive oxygen species (ROS) in the RVLM are increased in stroke-prone spontaneously hypertensive rats (SHRSP), which is a hypertensive rat model exhibiting increased SNA. We also demonstrated that the increase in SNA was due to ROS activation,[3] consistent with the findings of other studies.[4–6] Furthermore, oral administration of atorvastatin, an inhibitor of 3-hydroxy-3-methylglutaryl coenzyme A reductase, suppresses SNA probably through the inhibition of ROS in the RVLM of SHRSP.[7] Other studies suggest that central infusion of simvastatin suppresses SNA in heart failure models.[8–10] Our previous study was based on the oral administration of atorvastatin, however, and it is not known whether atorvastatin directly and chronically administered into the brain reduces the central sympathetic outflow via its effects on oxidative stress in the brain, particularly in the RVLM of hypertensive models.

In the brain, ROS are produced mainly through the activation of nicotinamide adenine dinucleotide phosphate [NAD(P)H] oxidase by the small G protein Rac1.[11,12] NAD(P)H oxidase is a multicomponent enzyme complex that comprises a membrane-bound heterodimer of gp91^{phox} (phagocytic oxidase) and p22^{phox}, and the cytosolic regulatory subunits p40^{phox}, p47^{phox}, p67^{phox}, and Rac1.[13–15] Transfection of dominant-negative Rac1 in the nucleus tractus solitarius decreases ROS and SNA.[12] Atorvastatin is also suggested to inhibit NAD(P)H oxidase activity in the vasculature,[16] the quadriceps muscle of diabetic rats,[17] and cardiomyocytes.[18] Furthermore, atorvastatin inhibits membrane translocation of Rac1, which is required for the activation of NAD(P)H oxidase in the vasculature.[16] In the kidney, rosuvastatin attenuates NAD(P)H oxidase activity through the inhibition of Rac1 and p22^{phox}.[18,19] In the brain, however, the contribution of atorvastatin to reducing ROS and its involvement in the inhibition of the membrane translocation of Rac1 and NAD(P)H oxidase activity is unknown. We previously demonstrated that Mn superoxide dismutase (SOD) activity is decreased in the RVLM of SHRSP, and the decrease contributes to the increase

Received for publication September 7, 2009; accepted November 10, 2009.
From the Department of Cardiovascular Medicine, Kyushu University Graduate School of Medical Sciences, Fukuoka, Japan.
This study was supported by a Grant-in-Aid for Scientific Research from the Japan Society for the Promotion of Science (B19390231).
The authors report no conflicts of interest.
Reprints: Yoshitaka Hirooka, MD, PhD, FAHA, Department of Cardiovascular Medicine, Kyushu University Graduate School of Medical Sciences, 3-1-1 Maidashi, Higashi-ku, Fukuoka 812-8582, Japan (e-mail: hyoshi@cardiol.med.kyushu-u.ac.jp).

in ROS.[3] A number of reports suggest that statins upregulate SOD in the vasculature.[20–23] Furthermore, the upregulation of Rac1 and NAD(P)H oxidase and the inhibition of SOD in the RVLM and nucleus tractus solitarius have major roles in increasing SNA and blood pressure (BP).[3,24] However, the mechanisms involved by which atorvastatin reduces ROS in the RVLM of SHRSP are not evaluated. The aim of the present study was thus to determine whether the sympathoinhibitory effect of atorvastatin due to the reduction of ROS in the RVLM is caused by the inhibition of Rac1-NAD(P)H oxidase activity and upregulation of Mn-SOD and Cu/Zn-SOD in the RVLM of SHRSP. Therefore, the aim of the present study was to examine the effects of atorvastatin administered into the brain and evaluate the changes in BP and SNA in SHRSP and to evaluate the oxidative stress and the NAD(P)H oxidase activity in the RVLM as the ROS generation. For this purpose, we determined the expression of Rac1, gp91^{phox}, and p22^{phox} in the membrane fraction and the expression of Rac1 and p40^{phox} in the cytosolic fraction of the RVLM. In addition, the activity of Cu/Zn-SOD, and Mn-SOD as scavenging enzymes of ROS was measured in the RVLM of intracerebroventricular (ICV) atorvastatin–treated and vehicle-infused SHRSP and Wistar Kyoto (WKY) rats.

MATERIALS AND METHODS

Animals and General Procedures

Male SHRSP/Izm rats and age-matched WKY rats (14–16 weeks old) were obtained from SLC Japan, Hamamatsu, Japan. Rats were fed a standard diet, and each strain was divided into 4 groups (SHRSP treated with atorvastatin, S-ATOR; SHRSP treated with vehicle, S-VEH; WKY treated with atorvastatin, W-ATOR; and WKY treated with vehicle, W-VEH; n = 5 per group). Atorvastatin (Pfizer, Inc, New York, NY) was dissolved in dimethyl sulfoxide and further diluted in artificial cerebrospinal fluid for a final concentration of 40 μg/mL. Atorvastatin or dimethyl sulfoxide in artificial cerebrospinal fluid was infused at 1 μL/h for 14 days with an osmotic minipump (Alzet 1003D; Alza Scientific Products, Palo Alto, CA) into the left lateral ventricle of the brain (from bregma: anteroposterior, −0.8 mm; lateral, 1.5 mm; and depth, 3.5 mm). The flow rate of agents in ICV methods was determined to have the significant effect in brainstem.[25] In a preliminary experiment, this dose of atorvastatin did not affect BP and heart rate (HR) when administered intravenously. Food and tap water were available ad libitum throughout the study. BP and HR were measured using the UA-10 radio-telemetry system (Data Science International, Dallas, TX) as described previously.[3,26–28] Urinary norepinephrine excretion (uNE) for 24 hours was calculated as an indicator of SNA, as described previously.[3,25–27] In addition, spectral analysis was performed using an adaptive autoregressive model to provide power spectra for systolic BP (SBP). Low frequency power of SBP was computed by integrating the spectra between 0.04 and 0.15 Hz, and SNA is presented as the normalized unit of the low frequency component of SBP (LFnuSBP).[29–31] Baroreflex sensitivity (BRS) was measured using the spontaneous sequence method as a parameter of autonomic control. Sequence analysis was performed to detect sequences of 3 or more beats in which there was either an increase in SBP and pulse interval (up sequence) or a decrease in SBP and pulse interval (down sequence). BRS was estimated as the mean slope of the up and down sequences.[32–34] The RVLM was defined according to a rat brain atlas as described previously.[3,26–28] The study protocol was reviewed and approved by the Committee on the Ethics of Animal Experiments at the Kyushu University Graduate School of Medical Sciences and conducted according to the Guidelines for Animal Experiments of Kyushu University.

Measurement of TBARS

The RVLM tissues were homogenized, and thiobarbituric acid (0.3%) was added to the homogenate. The mixture was extracted with a mixture of distilled water and *n*-butanolpyridine (15:1) and centrifuged at 1600*g* for 10 minutes. The amount of thiobarbituric acid reactive substances (TBARS) was determined by absorbance measured at 532 nm, as described previously.[3,7]

Expression of Rac1, gp91^{phox}, and p22^{phox} in the Membrane Fraction and Rac1, p47^{phox} and p40^{phox} in the Cytosolic Fraction

Western blot analysis was used to determine the expression of Rac1 (Upstate Biotechnology, Lake Placid, NY),[12] gp91^{phox}, and p22^{phox} in the membrane fraction (Santa Cruz Biotechnology, Santa Cruz, CA), and the expression of Rac1, p47^{phox}, and p40^{phox} in the cytosolic fraction (Santa Cruz Biotechnology, Santa Cruz, CA) of the RVLM.

Activity of Rac1 in the RVLM

Rac1 activity can be monitored by its interaction with p21-activated kinase, which only occurs when Rac1 is active. We used a Rac1 Activation kit (Upstate Biotechnology, Lake Placid, NY) to evaluate Rac1 activity in the RVLM, as previously described.[12]

NAD(P)H Oxidase Activity

NAD(P)H-dependent superoxide production in the RVLM was measured using a lucigenin luminescence assay as described previously.[35,36] Quantification of NAD(P)H oxidase activity was expressed relative to that in WKY rats, which was assigned a value of 1.

Cu/Zn-SOD and Mn-SOD Activity in the RVLM

Cu/Zn-SOD or Mn-SOD activity was assayed by monitoring the inhibition of the rate of xanthine-mediated/xanthine oxidase–mediated reduction of cytochrome c (pH 7.4). To discriminate between Cu/Zn-SOD and Mn-SOD activities, the assay was also performed after incubation in the presence of KCN, which selectively inhibits the Cu/Zn-SOD isoform.[37] Cu/Zn- and Mn-SOD activities were expressed relative to those in vehicle-treated WKY rats, which were assigned a value of 1.

Microinjection of Apocynin Into the Bilateral RVLM

In other S-ATOR and S-VEH, (n = 5 for each) on day 14, the NAD(P)H oxidase inhibitor apocynin (1 nmol) was microinjected bilaterally into the RVLM, as described previously.[3]

Statistical Analysis

Normally distributed variables were expressed as mean ± SD. An unpaired t test was used to compare the differences between groups of normally distributed variables, and the Mann–Whitney U test was used to compare differences between groups of non–normally distributed variables. A 2-factor repeated-measures analysis of variance was used to compare differences between groups. Differences were considered to be statistically significant with a P value of less than 0.05.

RESULTS

BP, HR, SNA, and BRS

Mean BP (MBP) and HR were significantly decreased on day 4 after the administration of atorvastatin in S-ATOR. On day 14, MBP, HR, 24-hour uNE, and LFnuSBP were significantly higher in S-VEH than in W-VEH and lower in S-ATOR than in S-VEH (Fig. 1A–D). BRS was significantly lower in S-VEH than in W-VEH (12.8 ± 2.3 vs. 19.7 ± 1.8 ms/mm Hg, n = 5 for each; $P < 0.05$) and significantly higher in S-ATOR than in S-VEH (16.4 ± 1.6 vs. 12.8 ± 2.3 ms/mm Hg, n = 5 for each; $P < 0.05$). Mean BP, HR, 24-hour uNE, LFnuSBP, and BRS values did not significantly differ between W-ATOR and W-VEH (Fig. 1A–D).

Oxidative Stress Measured by TBARS Methods in the RVLM

Oxidative stress in the RVLM measured by the TBARS method was significantly lower in S-ATOR than in S-VEH (Fig. 2). Oxidative stress did not differ significantly between W-ATOR and W-VEH (Fig. 2).

Activity of NAD(P)H Oxidase and Rac1 in the RVLM

The activity of NAD(P)H oxidase was significantly lower in S-ATOR than in S-VEH (Fig. 3A). The activity of Rac1 was also significantly lower in S-ATOR than in S-VEH (Fig. 3B). NAD(P)H oxidase activity and Rac1 activity did not significantly differ between W-ATOR and W-VEH (Fig. 3A, B).

Expression of Rac1, gp91^{phox}, and p22^{phox} in the Membrane Fraction and Rac1, p47^{phox}, and p40^{phox} in the Cytosolic Fraction

The expression of Rac1, gp91^{phox}, and p22^{phox} in the membrane fraction was significantly lower in S-ATOR than in S-VEH (Fig. 4A–C). The expression of p47^{phox} and p40^{phox} in the cytosolic fraction was also significantly lower in S-ATOR than in S-VEH (Fig. 5B, C). The expression of Rac1 in the cytosolic fraction was significantly higher, however, in S-ATOR than in S-VEH (Fig. 5A). The expression of Rac1, gp91^{phox}, and p22^{phox} in the membrane fraction and the expression of Rac1, p47^{phox}, and p40^{phox} in cytosolic fraction did not differ significantly between W-ATOR and W-VEH (Figs. 4A–C, 5A–C).

Cu/Zn- and Mn-SOD Activity in the RVLM

Mn-SOD activity in the RVLM was significantly higher in S-ATOR than in S-VEH, but Cu/Zn-SOD activity did not significantly differ between S-ATOR and S-VEH (Fig. 6A, B).

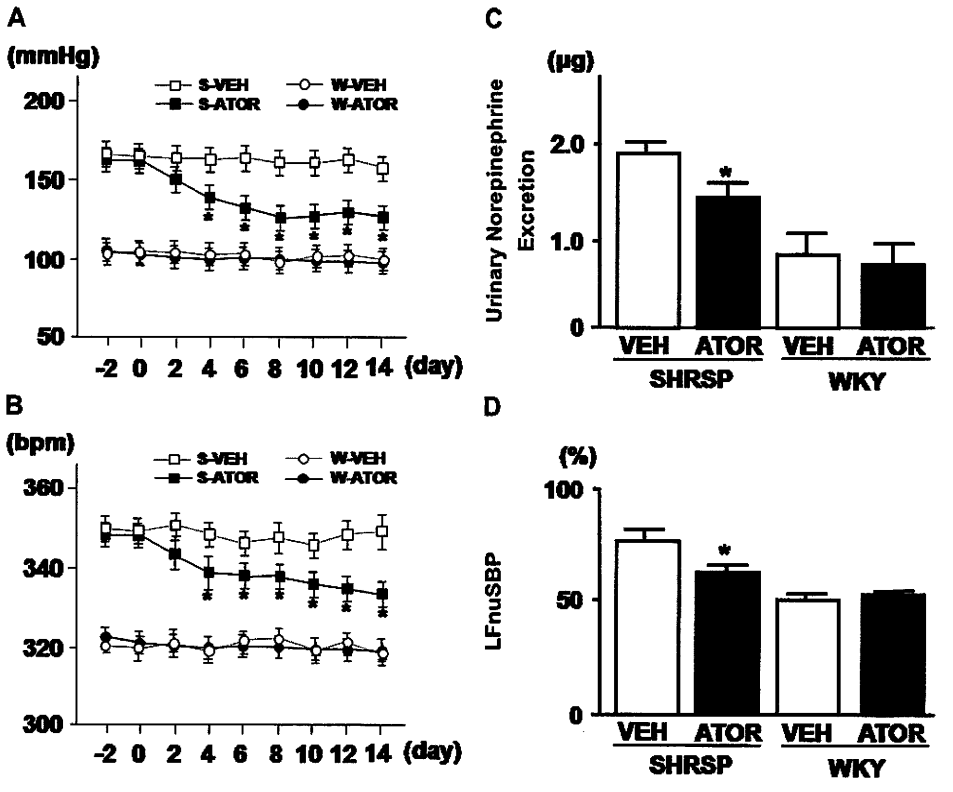

FIGURE 1. Time course of MBP (in mm Hg) (A) and HR (in beats per minute) (B) in S-ATOR (n = 5), S-VEH (n = 5), W-ATOR (n = 5), and W-VEH (n = 5). *$P < 0.05$ for ATOR versus VEH values in each strain. C, D, Urinary norepinephrine excretion for 24 hours (in micrograms) (C) and LFnuSBP (percentage) (D) at day 14 in ATOR- or VEH-treated SHRSP or WKY (n = 5 for each). *$P < 0.05$ for ATOR versus VEH values in each strain. †$P < 0.05$ compared with VEH-treated WKY. Data are shown as mean ± standard error of the mean.

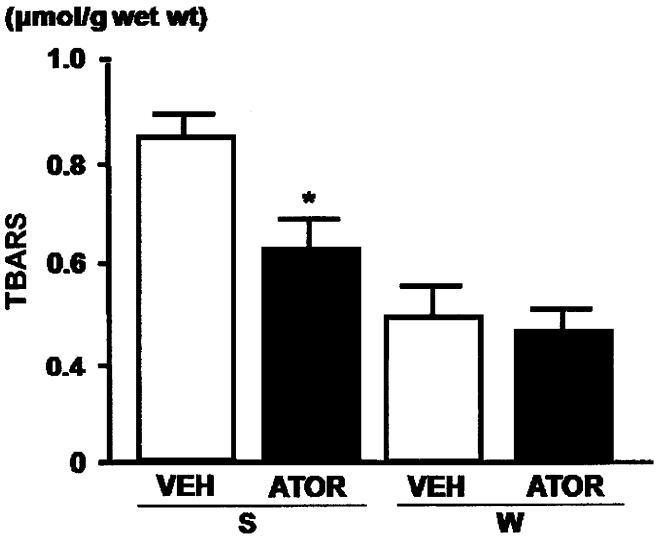

FIGURE 2. TBARS levels (in micromolars per gram wet weight) in the RVLM at day 14 in ATOR- or VEH-treated SHRSP or WKY (n = 5 for each). *$P < 0.05$ for ATOR versus VEH in each strain. †$P < 0.05$ compared with VEH-treated WKY. Data are shown as mean ± standard error of the mean.

Cu/Zn- and Mn-SOD activity did not significantly differ between W-ATOR and W-VEH (Fig. 6A, B).

Microinjection of Apocynin Into the RVLM

The degree of the change in MBP induced by the microinjection of apocynin into the bilateral RVLM was significantly smaller in S-ATOR than in S-VEH (−9.4 ± 1.9 vs. −26.4 ± 3.7 mm Hg; n = 5; $P < 0.05$).

DISCUSSION

The novel finding of the present study was that atorvastatin administered chronically into the brain in SHRSP reduced BP and SNA in SHRSP and that it was associated with reduced oxidative stress, probably due to the inhibition of NAD(P)H oxidase and the activation of Mn-SOD in the RVLM of SHRSP. This is supported by the following findings: (1) ICV injection of atorvastatin for 14 days decreased MBP, HR, SNA, and TBARS in the RVLM of SHRSP; (2) ICV injection of atorvastatin decreased NAD(P)H oxidase activity through the inhibition of Rac1 membrane translocation in the RVLM of SHRSP; (3) ICV injection of atorvastatin activated Mn-SOD in the RVLM of SHRSP; and (4) changes in MBP induced by microinjection of NAD(P)H oxidase inhibitor into the RVLM were significantly smaller in SHRSP treated with atorvastatin than in SHRSP treated with vehicle. Thus, atorvastatin inhibits Rac1 membrane translocation and Rac1 activity in the RVLM of SHRSP.

Atorvastatin decreased the expression of NAD(P)H membrane-bound subunits $gp91^{phox}$ and $p22^{phox}$ and the cytosolic regulatory subunit $p47^{phox}$ and $p40^{phox}$ and inhibited NAD(P)H oxidase activity in the RVLM of SHRSP. Oral administration of atorvastatin decreases ROS in the RVLM of SHRSP.[3] In the brain, ROS is produced mainly by NAD(P)H oxidase, which is activated through Rac1 membrane translocation.[11] In another area of the brainstem, the nucleus tractus solitarius, the inhibition of Rac1 decreases NAD(P)H oxidase activity and ROS formation.[12] Previous reports suggest that atorvastatin inhibits Rac1 membrane translocation and NAD(P)H oxidase activity in the vasculature of hypertensive rats.[13] We found that the depressor response elicited by apocynin into the RVLM was attenuated in SHRSP treated with ICV atorvastatin in the present study. Based on these findings, we suggest that the atorvastatin-induced reduction of ROS in the RVLM of SHRSP is caused by a decrease in NAD(P)H oxidase activity linked to the inhibition of Rac1 membrane translocation.

Atorvastatin activated Mn-SOD activity in the RVLM of SHRSP but not Cu/Zn-SOD. In the RVLM of SHRSP, Mn-SOD activity is decreased, and overexpression of Mn-SOD in the RVLM of SHRSP decreases ROS.[3] A number of reports suggest that statins activate total SOD[20–23] and Cu/Zn-SOD in the vasculature.[26,27] In the present study, however, atorvastatin did not activate Cu/Zn-SOD in the RVLM of SHRSP. In the nucleus tractus solitarius, Cu/Zn-SOD expression is decreased in SHRSP.[26] It is not clear why atorvastatin did not activate Cu/Zn-SOD in the present study. Recently, we reported that angiotensin II increases the intracellular Ca^{2+} concentration and that the increase in mitochondrial Ca^{2+} uptake leads to mitochondrial ROS production in the RVLM.[24] Therefore, it is possible that atorvastatin-induced activation of Mn-SOD in the RVLM of SHRSP contributes to inhibit ROS to an even greater extent than Cu/Zn-SOD.

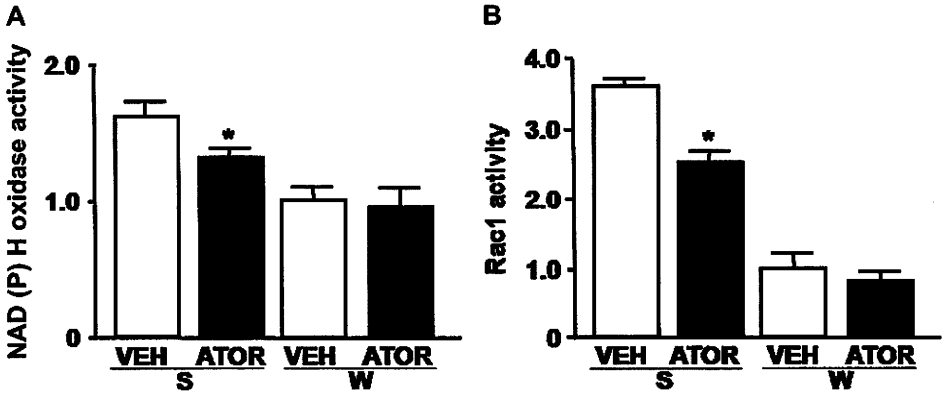

FIGURE 3. NAD(P)H oxidase activity (A) and Rac1 activity (B), in the RVLM at day 14 in ATOR- or VEH-treated SHRSP or WKY (n = 5 for each). *$P < 0.05$ for ATOR versus VEH in each strain. †$P < 0.05$ compared with VEH-treated WKY. NAD(P)H oxidase or Rac1 activity was expressed relative to that in W-VEH, which was assigned a value of 1. Data are shown as mean ± standard error of the mean.

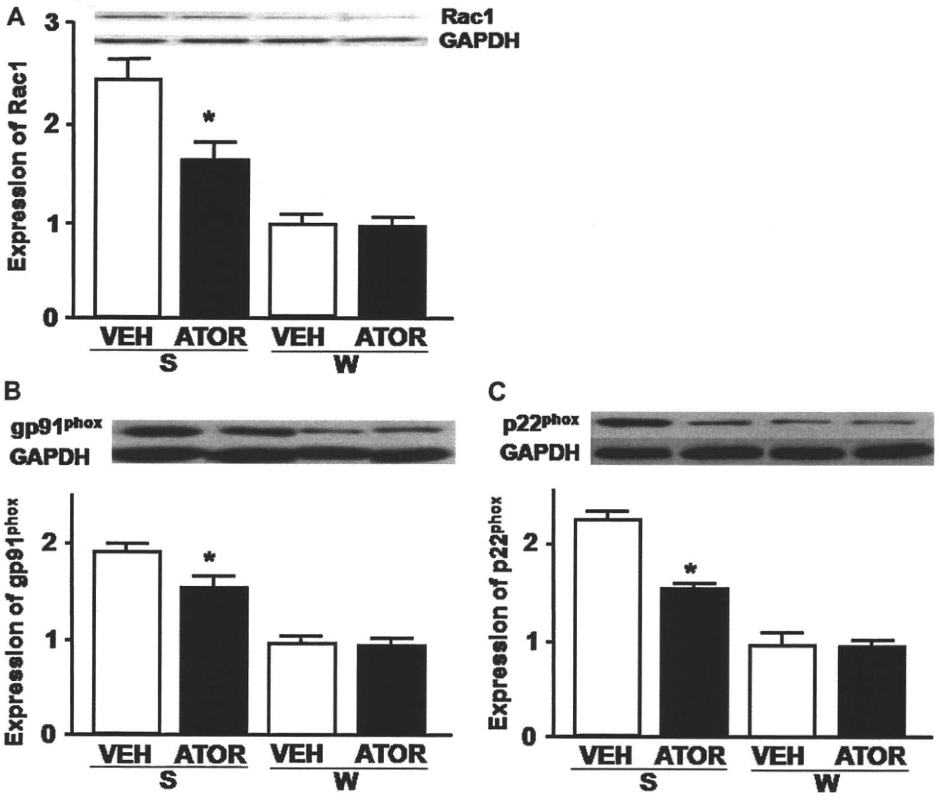

FIGURE 4. Western blot analysis showing the level of expression of Rac1 (A), gp91^{phox} (B), and p22^{phox} (C) in the membrane fraction of the RVLM at day 14 in ATOR- or VEH-treated SHRSP or WKY (n = 5 for each). *$P < 0.05$ for ATOR versus VEH in each strain. †$P < 0.05$ compared with VEH-treated WKY. The expression level of Rac1, gp91^{phox}, and p22^{phox} was expressed relative to that in W-VEH, which was assigned a value of 1. Data are shown as mean ± standard error of the mean.

In the present study, we measured SNA by spectral analysis. Low frequency power of SBP was computed by integrating the spectra between 0.04 and 0.15 Hz, and SNA is presented as LFnuSBP, as described in previous reports.[29–31] On day 14, the LFnuSBP values were comparable to those of uNE. Therefore, this method seems to be useful for measuring SNA in awake animals. Furthermore, atorvastatin improved the impaired baroreflex control in the SHRSP in the present study. Whereas we did not measure cardiac output in the present study and the reduction of BP and HR due to atorvastatin might cause a potential fall in cardiac output, the effects of atorvastatin are due to the decrease in sympathetic nerve activity. It is generally accepted that SNA is enhanced in SHRSP,[3,5,26–28,40] and atorvastatin attenuates the enhanced central sympathetic outflow to various organs including heart, kidney, and vasculature. At least, atorvastatin did not induce heart failure due to low cardiac output. We consider that the decrease in central sympathetic outflow reduced the peripheral vascular resistance by which cardiac output keep constant instead of the reduction of sympathetic outflow to the heart.

Another intriguing finding of the present study is that the BP-lowering and sympathoinhibitory effects are comparable between oral administration (50 mg/kg^{-1}/day^{-1})[7] and ICV injection (2 μg/kg^{-1}/day^{-1}) of atorvastatin. We confirmed the direct effects of atorvastatin administered into the brain on BP, SNA, and baroreflex function in SHRSP as one of the hypertensive models in the present study. The changes in TBARS levels are also similar between oral administration and ICV injection of atorvastatin. In SHRSP, the blood–brain barrier might be disrupted[38] and oral administration of atorvastatin is considered to affect the brain directly.[39] The present findings suggest that orally administered atorvastatin crosses the blood–brain barrier and affects the brain of SHRSP. The abnormal activation of sympathetic nervous system causes hypertension, heart failure, and ischemic heart diseases, and we consider that oral administration of atorvastatin has a potential to treat cardiovascular diseases due to the sympathoinhibition through the antioxidant effect in the RVLM.

We previously demonstrated that oral administration of atorvastatin increases the expression of endothelial nitric oxide synthase (eNOS) in the brainstem.[40] Overexpression of eNOS in the RVLM decreases SNA in WKY and SHRSP.[26–28] In the present study, we did not investigate whether an increase in NO production in the RVLM is involved in the reduction of BP and oxidative stress. It is possible, however, that ICV injection of atorvastatin increases eNOS in the RVLM of SHRSP and that an increase in eNOS contributes to the sympathoinhibitory effect. Further study is needed to clarify this issue.

In WKY rats, atorvastatin does not alter SNA and oxidative stress in the RVLM; these results are compatible with our previous report.[7] Moreover, atorvastatin also does not alter Rac1-induced NAD(P)H oxidase activity and Mn-SOD activity in the RVLM of WKY rats. In the present study, the mechanisms by which atorvastatin affected Rac1-induced NAD(P)H oxidase activity and Mn-SOD activity in SHRSP, but not in WKY, were not determined. It may be that there are thresholds for the induction of Rac1-induced NAD(P)H oxidase activity and Mn-SOD activity in the RVLM, which

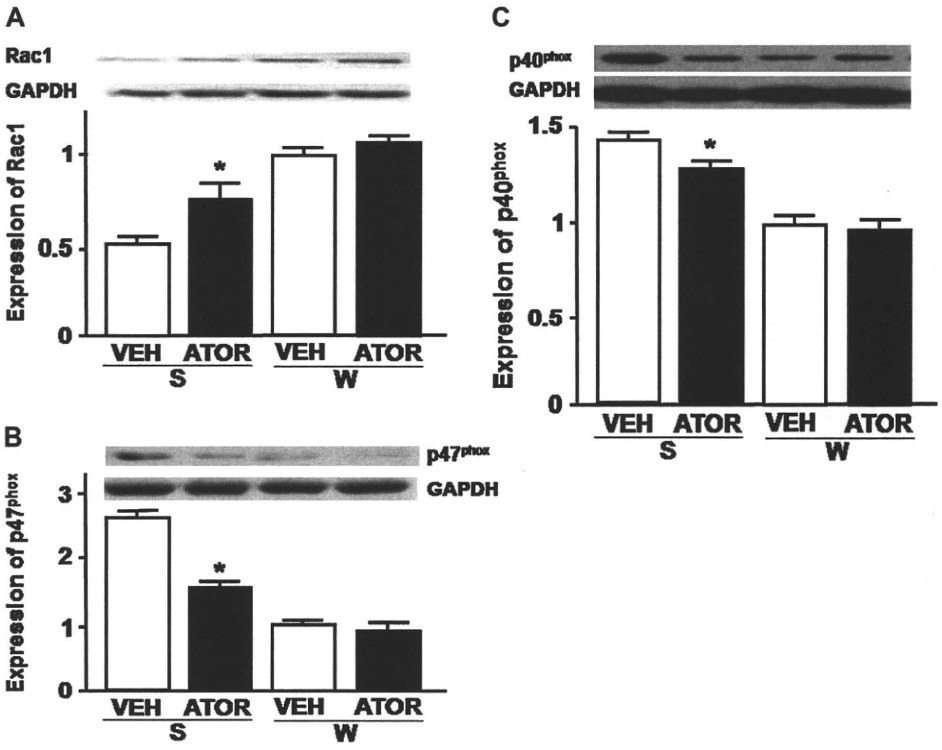

FIGURE 5. Western blot analysis showing the level of expression of Rac1 (A), $p47^{phox}$ (B), and $p40^{phox}$ (C) in the cytosolic fraction of the RVLM at day 14 in ATOR- or VEH-treated SHRSP or WKY (n = 5 per group). $*P < 0.05$ for ATOR versus VEH in each strain. $\dagger P < 0.05$ compared with VEH-treated WKY. The expression level of Rac1, $p47^{phox}$, and $p40^{phox}$ was expressed relative to that in W-VEH, which was assigned a value of 1. Data are shown as mean ± standard error of the mean.

are differently affected by atorvastatin between SHRSP and WKY rats.

STUDY LIMITATIONS

The present study has several limitations. First, we examined the effects of atorvastatin specifically in only the RVLM, and its effects in other brain areas cannot be excluded at this time. Nevertheless, neural activity in the RVLM has a direct influence on SNA,[1,2] and the present results identified an antioxidant effect of atorvastatin and its mechanisms in the RVLM. Angiotensin II type 1 receptors (AT_1R) are abundantly distributed in the RVLM, and there is a close link between AT_1R stimulation and NAD(P)H oxidase activation.[41] Therefore, in the present study, we focused on the RVLM, although other brain regions related to central autonomic control also contain AT_1R and NAD(P)H oxidase. Second, among all statins, we only studied the effect of atorvastatin, which is a lipophilic statin.[42] Our previous studies suggested that oral atorvastatin also reduces oxidative stress in the RVLM.[7] Further study is needed to clarify whether our results in the present study are broad class effects or are specific for atorvastatin. Finally, a recent study suggests that statins reduce BP in patients with hypertension.[43] It will be important to determine whether atorvastatin has this beneficial effect caused by the mechanism related to our suggestion in the present study, although we understand that this is difficult to examine in humans.

CONCLUSIONS

In conclusion, atorvastatin administered directly into the brain of SHRSP decreases BP, SNA, and baroreflex function. The findings of the present study suggest that these effects are associated with inhibition of oxidative stress in the RVLM, probably resulting from a decrease in NAD(P)H oxidase activity and the upregulation of Mn-SOD activity in the RVLM.

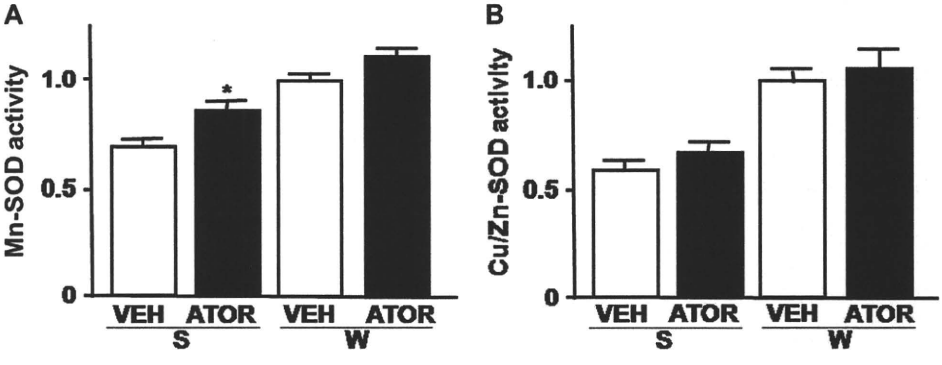

FIGURE 6. The activities of Mn-SOD (A) and Cu/Zn-SOD (B) in the RVLM at day 14 in ATOR- or VEH-treated SHRSP or WKY (n = 5 for each). $*P < 0.05$ for ATOR versus VEH in each strain. $\dagger P < 0.05$ compared with VEH-treated WKY. The activities of Mn-SOD and Cu/Zn-SOD were expressed relative to that in W-VEH, which was assigned a value of 1. Data are shown as mean ± standard error of the mean.

ACKNOWLEDGMENTS

We are grateful to Pfizer, Inc for supplying atorvastatin.

REFERENCES

1. Dampney RAL. Functional organization of central pathways regulating the cardiovascular system. *Physiol Rev.* 1994;74:323–364.
2. Guyenet PG. The sympathetic control of blood pressure. *Nat Rev Neurosci.* 2006;7:335–346.
3. Kishi T, Hirooka Y, Kimura Y, et al. Increased reactive oxygen species in rostral ventrolateral medulla contribute to neural mechanisms of hypertension in stroke-prone spontaneously hypertensive rats. *Circulation.* 2004;109:2357–2362.
4. Peterson JR, Sharma RV, Davisson RL. Reactive oxygen species in the neuropathogenesis of hypertension. *Curr Hypertens Rep.* 2006;8:232–241.
5. Hirooka Y. Role of reactive oxygen species in brainstem in neural mechanisms of hypertension. *Auton Neurosci.* 2008;142:20–24.
6. Sheh YL, Hsu C, Chan SHH, et al. NADPH oxidase- and mitochondrion-derived superoxide at rostral ventrolateral medulla in endotoxin-induced cardiovascular depression. *Free Radic Biol Med.* 2007;42:1610–1623.
7. Kishi T, Hirooka Y, Shimokawa H, et al. Atorvastatin reduces oxidative stress in the rostral ventrolateral medulla of stroke-prone spontaneously hypertensive rats. *Clin Exp Hypertens.* 2008;30:3–11.
8. Pliquett RU, Cornish KG, Peuler JD, et al. Simvastatin normalizes autonomic neural control in experimental heart failure. *Circulation.* 2003; 107:2493–2498.
9. Gao L, Wang W, Li YL, et al. Simvastatin therapy normalizes sympathetic neural control in experimental heart failure: roles of angiotensin II type 1 receptors and NAD(P)H oxidase. *Circulation.* 2005;112:1763–1770.
10. Gao L, Wang W, Zucker IH. Simvastatin inhibits central sympathetic outflow in heart failure by a nitric-oxide synthase mechanism. *J Pharmacol Exp Ther.* 2008;326:278–285.
11. Zimmerman MC, Dunlay RP, Lazartigues E, et al. Requirement for Rac1-dependent NADPH oxidase in the cardiovascular and dipsogenic actions of angiotensin II in the brain. *Circ Res.* 2004;95:532–539.
12. Nozoe M, Hirooka Y, Koga Y, et al. Inhibition of Rac1-derived reactive oxygen species in NTS decreases blood pressure and heart rate in stroke-prone SHR. *Hypertension.* 2007;50:62–68.
13. Byrne JA, Grieve DJ, Bendall JK, et al. Contrasting roles of NADPH oxidase isoforms in pressure-overload versus angiotensin II-induced cardiac hypertrophy. *Circ Res.* 2003;93:802–805.
14. Privratsky JR, Wold LE, Sowers JR, et al. AT1 blockade prevents glucose-induced cardiac dysfunction in ventricular myocytes: role of the AT1 receptor and NADPH oxidase. *Hypertension.* 2003;42:206–212.
15. Maach C, Kartes T, Killer H. Oxygen free radical release in human failing myocardium is associated with increased activity of Rac1-GTPase and represents a target for statin treatment. *Circulation.* 2003;108:1567–1574.
16. Wassmann S, Laufs U, Muller K, et al. Cellular antioxidant effects of atorvastatin in vitro and in vivo. *Arterioscler Thromb Vasc Biol.* 2002;22: 300–305.
17. Riad A, Du J, Stiehl S, et al. Low-dose treatment with atorvastatin leads to anti-oxidative and anti-inflammatory effects in diabetes mellitus. *Eur J Pharmacol.* 2007;569:204–211.
18. Habibi J, Whaley-Connell A, Qazi MA, et al. Rosuvastatin, a 3-hydroxy-3-methylglutaryl coenzyme A reductase inhibitor, decreases cardiac oxidative stress and remodeling in Ren2 transgenic rats. *Endocrinology.* 2007;148:2181–2188.
19. Whaley-Connell A, Habibi J, Nistala R, et al. Attenuation of NADPH oxidase activation and glomerular filtration barrier remodeling with statin treatment. *Hypertension.* 2008;51:474–480.
20. Chen X, Touyz RM, Park JB, et al. Antioxidant effects of vitamin C and E are associated with altered activation of vascular NADPH oxidase and superoxide dismutase in stroke-prone SHR. *Hypertension.* 2001;38: 606–611.
21. Carneado J, Alvarez de Sotomayor M, Perez-Guerrero C, et al. Simvastatin improves endothelial function in spontaneously hypertensive rats through a superoxide dismutase mediated antioxidant effect. *J Hypertens.* 2002;20:429–437.
22. Yilmaz MI, Baykal Y, Kilic M, et al. Effects of statins on oxidative stress. *Biol Trace Elem Res.* 2004;98:119–127.
23. Umeji K, Umemoto S, Itoh S, et al. Comparative effects of pitavastatin and probucol on oxidative stress, Cu/Zn superoxide dismutase, PPAR-gamma, and aortic stiffness in hypercholesterolemia. *Am J Physiol.* 2006;291: H2522–H2532.
24. Nozoe M, Hirooka Y, Koga Y, et al. Mitochondria-derived reactive oxygen species mediate sympathoexcitation induced by angiotensin II in the rostral ventrolateral medulla. *J Hypertens.* 2008;26:2176–2184.
25. Nishimura M, Takahashi H, Yoshimura M. Upregulation of the brain renin-angiotensin system in rats with chronic renal failure. *Acta Physiol (Oxf).* 2007;189:369–377.
26. Kishi T, Hirooka Y, Sakai K, et al. Overexpression of eNOS in the RVLM causes hypotension and bradycardia via GABA release. *Hypertension.* 2001;38:896–901.
27. Kishi T, Hirooka Y, Ito K, et al. Cardiovascular effects of overexpression of endothelial nitric oxide synthase in the rostral ventrolateral medulla in stroke-prone spontaneously hypertensive rats. *Hypertension.* 2002;39: 264–268.
28. Kishi T, Hirooka Y, Kimura Y, et al. Overexpression of eNOS in RVLM improves impaired baroreflex control of heart rate in SHRSP. *Hypertension.* 2003;41:255–260.
29. Castiglioni P, Di Rienzo M, Veicsteinas A, et al. Mechanisms of blood pressure and heart rate variability: an insight from low-level paraplegia. *Am J Physiol.* 2007;292:R1502–R1509.
30. Cerutti C, Gustin MP, Paultre CZ. Autonomic nervous system and cardiovascular variability in rats: a spectral analysis approach. *Am J Physiol.* 1991;261:H1292–H1299.
31. Pagani M, Montano N, Porta A, et al. Relationship between spectral components of cardiovascular variabilities, and direct measures of muscle sympathetic nerve activity in humans. *Circulation.* 1997;95:1441–1448.
32. Waki H, Kasparov S, Wong LF, et al. Chronic inhibition of eNOS activity in nucleus tractus solitarii enhances baroreceptor reflex in conscious rats. *J Physiol.* 2003;546:233–242.
33. Waki H, Katahira K, Polson JW, et al. Automation of analysis of cardiovascular autonomic function from chronic measurements of arterial pressure in conscious rats. *Exp Physiol.* 2006;91:201–213.
34. Braga VA, Burmeister MA, Sharma RV, et al. Cardiovascular responses to peripheral chemoreflex activation and comparison of different methods to evaluate baroreflex gain in conscious mice using telemetry. *Am J Physiol.* 2008;295:R1168–R1174.
35. Tai MH, Wang LL, Wu KL, et al. Increased superoxide anion in rostral ventrolateral medulla contributes to hypertension in spontaneously hypertensive rats via interactions with nitric oxide. *Free Radic Biol Med.* 2005;38:450–462.
36. Tanaka M, Umemoto S, Kawahara S, et al. Angiotensin II type 1 receptor antagonist and angiotensin-converting enzyme inhibitor altered the activation of Cu/Zn-containing superoxide dismutase in the heart of stroke-prone spontaneously hypertensive rats. *Hypertens Res.* 2005;28: 67–77.
37. Romero RM, Canuelo A, Lara EM, et al. Aging affects but does not eliminate the enzymatic antioxidative response to hypoxia/reoxygenation in cerebral cortex. *Exp Gerontol.* 2006;41:25–31.
38. Iwanaga Y, Ueno M, Ueki M, et al. The expression of osteopontin is increased in vessels with blood-brain barrier impairment. *Neuropathol Appl Neurobiol.* 2008;34:145–154.
39. Cibickova L, Radomir H, Stanislav M, et al. The influence of simvastatin, atorvastatin and high-cholesterol diet on acetylcholinesterase activity, amyloid beta and cholesterol synthesis in rat brain. *Steroids.* 2009;74: 13–19.
40. Kishi T, Hirooka Y, Mukai Y, et al. Atorvastatin causes depressor and sympatho-inhibitory effects with upregulation of nitric oxide synthases in stroke-prone spontaneously hypertensive rats. *J Hypertens.* 2003;21: 379–386.
41. Hu L, Zhu DN, Yu Z, et al. Expression of angiotensin II type 1 (AT1) receptor in the rostral ventrolateral medulla in rats. *J Appl Physiol.* 2002; 92:2153–2161.
42. Cibickova L, Hyspler R, Ticha A, et al. Cholesterol synthesis in central nervous system of rat is affected by simvastatin as well as by atorvastatin. *Pharmazie.* 2008;63:819–822.
43. Golomb BA, Dimsdale JE, White HL, et al. Reduction in blood pressure with statins: results from the USCD Statin Study, a randomized trial. *Arch Intern Med.* 2008;168:721–727.

Para-Hisian Pacing for a Pediatric Patient with a Congenitally Corrected Transposition of the Great Arteries (SLL)

MASAO TAKEMOTO, M.D.,*,§ ATSUHIRO NAKASHIMA, M.D.,†,§
JUN MUNEUCHI, M.D.,‡,§ KEN-ICHIRO YAMAMURA, M.D.,‡,§
YUICHI SHIOKAWA, M.D.,†,§ KENJI SUNAGAWA, M.D.,* and RYUJI TOMINAGA, M.D.†
From the *Department of Cardiovascular Medicine, †Department of Cardiovascular Surgery, and ‡Department of Pediatrics, Heart Center, Kyushu University Hospital, Fukuoka, Japan

We report a pediatric patient with a congenitally corrected transposition of the great arteries (ccTGA)(SLL) in which permanent para-Hisian pacing (PPHP) could improve dyssynchrony-associated systemic ventricular (SV) dysfunction resulting from permanent morphologic left ventricular pacing for complete atrioventricular block. Since, in patients with ccTGA(SLL), an elongated His-bundle runs medially toward the upper septum to the site of the fibrous continuity between the right-sided mitral valve and pulmonary artery, the His-bundle may easily be captured by a pacing lead, unlike in normal hearts. Thus, PPHP may be an effective therapeutic strategy for the treatment of dyssynchrony-associated SV dysfunction associated with ccTGA (SLL). (PACE 2010; 33:e4–e7)

transposition of the great arteries, para-Hisian pacing, heart failure, cardiac resynchronization therapy, pediatrics, dyssynchrony

Introduction

The cardiac-resynchronization therapy (CRT) utilizing tranvenous biventricular pacing has become proven to produce clinical benefits in adult[1] and pediatric[2] patients with dyssynchrony-associated systemic ventricular (SV) dysfunction. Here, we report a case of prevention of ventricular desynchronization, so-called cardiac resynchronization, by utilizing transvenous permanent para-Hisian pacing (TPPHP) for dyssynchrony-associated SV dysfunction resulting from permanent morphologic left ventricular (mLV) pacing for complete atrioventricular (AV) block (CAVB) in a pediatric patient with a congenitally corrected transposition of the great arteries (ccTGA)(SLL).

Case Report

An 8-year-old girl was admitted to our hospital with a chief complaint of general fatigue and impaired daily life activities under appropriate medication with an angiotensin II receptor blocker, β-adrenergic receptor blocker, and diuretics. She had a history of repeated cardiac surgeries, consisting of a pulmonary artery banding for ccTGA(SLL), and coexisting anomalies involving an atrial septal defect (ASD) and ventricular septal defect (VSD) at a month after her birth (Fig. 1A), and the implantation of permanent epicardial pacing leads into the right atrium (RA), mLV, and SV, respectively, for CAVB following both an ASD and VSD closure at the age of 1 year (Figs. 1B and 2). The pulse generator was implanted in the intraperitoneum. Although the mLV and RA leads were still functional, the SV lead had already fractured (Fig. 2).

On admission, her blood pressure was 96/58 mmHg, and auscultation revealed a significant regurgitant systolic murmur. The electrocardiogram (ECG) revealed all ventricular pacing with a prolonged QRS duration following the intrinsic P wave (Fig. 1C). Chest X-rays revealed cardiomegaly with a 60% cardio-thoracic ratio. Her initial two-dimensional and Doppler echocardiography (UCG) revealed a severe dyssynchronous SV (morphologic RV) contraction with an SV dilation, reduced SV ejection fraction (SVEF = 19%), and severe left-sided AV (tricuspid, left) valvular regurgitation (Table I). The serum brain natriuretic peptide (BNP) was elevated to 263 pg/dL. Since we presumed the permanent mLV pacing might contribute to her SV dysfunction and heart failure (HF) progression, with left-sided AV valve regurgitation, preventative therapy with ventricular desynchronization was considered. We performed TPPHP for prevention of ventricular desynchronization, following an electrophysiological study, under general anesthesia. The bipolar screw-in leads were advanced via the left subclavian vein

There are no conflicts of interest that are related to the manuscript.

§ Contributed equally to this paper.

Address for reprints: Masao Takemoto, M.D., Ph.D., Department of Cardiovascular Medicine, Kyushu University Hospital, 3-1-1 Maidashi, Higashi-ku, Fukuoka 812-8582, Japan. Fax: 81-92-642-5374; e-mail: matakemo@cardiol.med.kyushu-u.ac.jp

Received February 20, 2009; revised March 31, 2009; accepted May 10, 2009.

doi: 10.1111/j.1540-8159.2009.02559.x

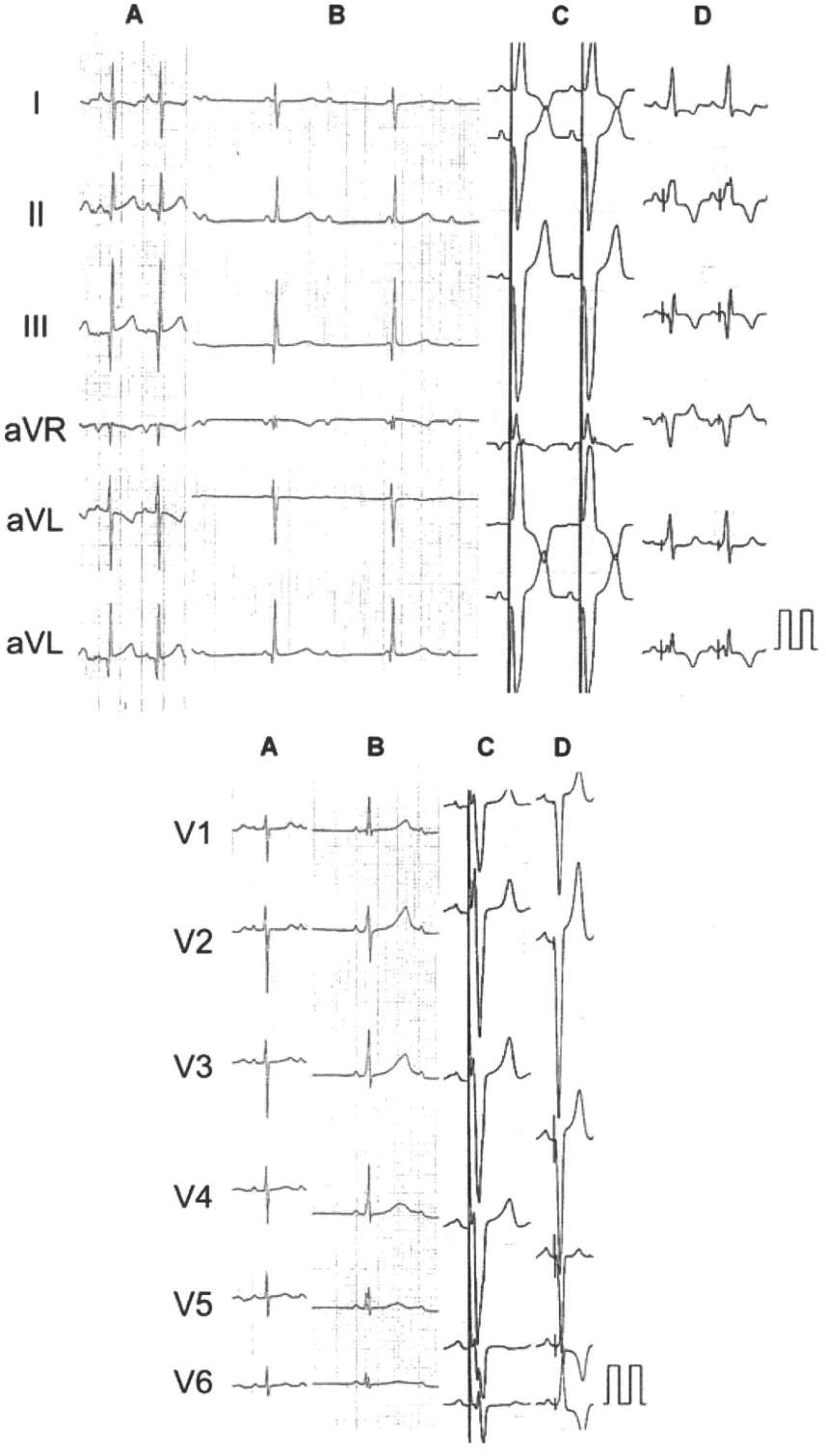

Figure 1. *The electrocardiogram during sinus rhythm at a month after her birth (A), during complete atrioventricular block at an age of 1 year (B), during epicardial morphologic left ventricular pacing on admission (QRS duration = 198 ms)(C), and during para-Hisian pacing (QRS duration = 94 ms)(D).*

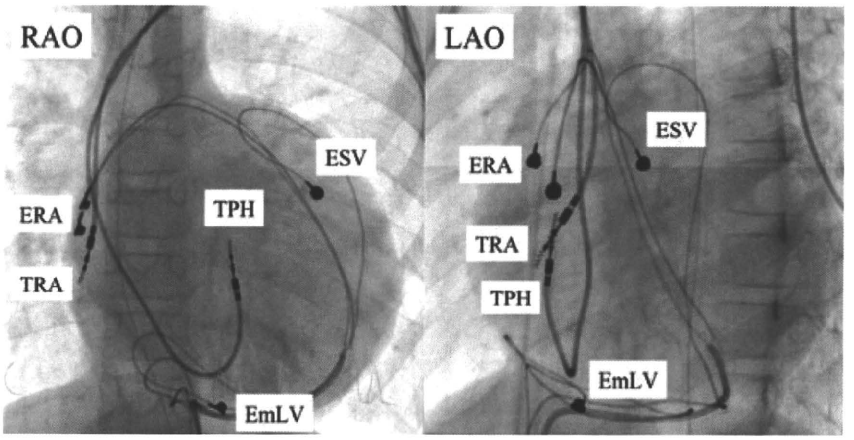

Figure 2. *Fluoroscopic images in the right (left panel) and left (right panel) anterior oblique (RAO and LAO) views. The EmLV, ERA, and ESV indicate the epicardial lead(s) in the morphologic left ventricle, right atrium, and systemic ventricle, respectively. The TPH and TRA indicate the transvenous para-Hisian pacing and transvenous right atrial leads, respectively.*

and easily positioned, using a steerable stylet into the para-His-bundle in the interventricular septum (Medtronic 5076-58, Medtronic Japan Co., Ltd, Tokyo, Japan) and RA (Medtronic 5076-52), respectively (Fig. 2), with the pulse generator (Guidant INSIGNIA I Plus DR, Guidant Japan KK, Tokyo, Japan) placed in the upper area anterior to the pectoralis major muscle of the left chest, as previously described.[3] Further, the pulse generator implanted in the intraperitoneum was turned off thereafter. The pacing threshold of the para-His-bundle lead was 0.7 Volt. The AV delay was optimized at 120 ms by UCG. TPPHP exhibited a concordant QRS axis with a native QRS (Fig. 1A and D), and could dramatically shorten the QRS duration of the ECG (Fig. 1C and D) and decrease the degree of left-sided AV valvular regurgitation as determined by UCG in accordance with an improvement in the dyssynchronous SV contraction (Table I). These conditions met the requirements of a successful criteria for TPPHP as previously defined.[4] Finally, her daily life activities steadily improved thereafter. Six months after the procedures, her clinical status, cardiomegaly, SVEF, dyssynchronous SV contraction, and serum BNP level all improved (Table I).

Discussion

Recent clinical trials have revealed that permanent right ventricular pacing could promote a dyssynchronous ventricular contraction leading to SV dysfunction and HF progression in adult patients,[5] and also contribute to adverse histological remodeling and eventual contractile dysfunction in pediatric patients.[6] A previous clinical study demonstrated that TPPHP may be one therapeutic strategy for the prevention of ventricular desynchronization in adult patients.[4]

In patients with ccTGA(SLL), the AV node is located well outside Koch's triangle, typically in an anterior and slightly lateral location within the RA, and an elongated His-bundle runs

Table I.

Parameters before and after Para-Hisian Pacing

	Before	After
Echocardiographical evaluation		
Systemic ventricular ejection fraction (%)	19	25
End-diastolic diameter of the systemic ventricle (mm)	64	63
Left-sided atrioventricular valve regurgitation (degree)	4	1
Interventricular delay[8] (milliseconds)	137	37
Other parameters		
QRS duration of the electrocardiogram (milliseconds)	198	94
New York Heart Association functional class	III	II
Serum brain natriuretic peptide (pg/dl)	263	151
Cardio-thoracic ratio (%)	60	53

Before, before para-Hiscian pacing; After, 6-months after para-Hiscian pacing
The interventricular delay was calculated by echocardiography, as previously described.[8]

medially toward the upper septum to the site of the fibrous continuity between the right-sided mitral valve and pulmonary artery in that region.[7] Thus, the His-bundle may easily be captured by a pacing lead unlike that in normal hearts. At present, the main limiting factor of the transvenous implantation of pacing leads in children may be the existence of the possible risk of a pacing lead distension and/or dislodgment associated with the patients' growth. It was suggested that such risk would be low, since these patients may have a slightly shorter stature; however, TPPHP may be prone to scarring and there are no long-term data on these leads, especially in children.

Thus, we performed TPPHP for prevention of ventricular desynchronization in this present case. It dramatically improved the dyssynchronous SV contraction and clinical status (Table I). In view of these findings, TPPHP may be one of the effective therapeutic strategies for the treatment of dyssynchrony-associated SV dysfunction and HF progression with ccTGA(SLL). Supporting data from large clinical trials, however, are needed before such conclusions can be made.

Acknowledgements: We thank John Martin for his linguistic assistance with this paper.

References

1. Abraham WT, Fisher WG, Smith AL, Delurgio DB, Leon AR, Loh E, Kocovic DZ, et al. Cardiac resynchronization in chronic heart failure. N Engl J Med 2002; 346:1845–1853.
2. Dubin AM, Janousek J, Rhee E, Strieper MJ, Cecchin F, Law IH, Shannon KM, et al. Resynchronization therapy in pediatric and congenital heart disease patients: An international multicenter study. J Am Coll Cardiol 2005; 46:2277–2283.
3. Deshmukh PM, Romanyshyn M. Direct His-bundle pacing: Present and future. Pacing Clin Electrophysiol 2004; 27:862–870.
4. Occhetta E, Bortnik M, Magnani A, Francalacci G, Piccinino C, Plebani L, Marino P. Prevention of ventricular desynchronization by permanent para-Hisian pacing after atrioventricular node ablation in chronic atrial fibrillation: A crossover, blinded, randomized study versus apical right ventricular pacing. J Am Coll Cardiol 2006; 47:1938–1945.
5. Sweeney MO, Hellkamp AS, Ellenbogen KA, Greenspon AJ, Freedman RA, Lee KL, Lamas GA. Adverse effect of ventricular pacing on heart failure and atrial fibrillation among patients with normal baseline QRS duration in a clinical trial of pacemaker therapy for sinus node dysfunction. Circulation 2003; 107:2932–2937.
6. Karpawich PP. Chronic right ventricular pacing and cardiac performance: The pediatric perspective. Pacing Clin Electrophysiol 2004; 27:844–849.
7. Anderson RH, Arnold R, Wilkinson JL. The conducting system in congenitally corrected transposition. Lancet 1973; 1:1286–1288.
8. Jauvert G, Rousseau-Paziaud J, Villain E, Iserin L, Hidden-Lucet F, Ladouceur M, Sidi D. Effects of cardiac resynchronization therapy on echocardiographic indices, functional capacity, and clinical outcomes of patients with a systemic right ventricle. Europace 2008.

Am J Physiol Heart Circ Physiol 298: H1966–H1975, 2010.
First published March 26, 2010; doi:10.1152/ajpheart.00340.2009.

Parallel resetting of arterial baroreflex control of renal and cardiac sympathetic nerve activities during upright tilt in rabbits

Atsunori Kamiya, Toru Kawada, Masaki Mizuno, Shuji Shimizu, and Masaru Sugimachi
Department of Cardiovascular Dynamics, National Cardiovascular Centre Research Institute, Suita, Japan

Submitted 8 April 2009; accepted in final form 23 March 2010

Kamiya A, Kawada T, Mizuno M, Shimizu S, Sugimachi M. Parallel resetting of arterial baroreflex control of renal and cardiac sympathetic nerve activities during upright tilt in rabbits. *Am J Physiol Heart Circ Physiol* 298: H1966–H1975, 2010. First published March 26, 2010; doi:10.1152/ajpheart.00340.2009.—Since humans are under ceaseless orthostatic stress, the mechanisms to maintain arterial pressure (AP) against gravitational fluid shift are important. As one mechanism, it was reported that upright tilt reset baroreflex control of renal sympathetic nerve activity (SNA) to a higher SNA in anesthetized rabbits. In the present study, we tested the hypothesis that upright tilt causes a parallel resetting of baroreflex control of renal and cardiac SNAs in anesthetized rabbits. In anesthetized rabbits (n = 8, vagotomized and aortic denervated) with 0° supine and 60° upright tilt postures, renal and cardiac SNAs were simultaneously recorded while isolated intracarotid sinus pressure (CSP) was increased stepwise from 40 to 160 mmHg with increments of 20 mmHg. Upright tilt shifted the reverse-sigmoidal curve of the CSP-SNA relationship to higher SNA similarly in renal and cardiac SNAs. Although upright tilt increased the maximal gain, the response range and the minimum value of SNA, the curves were almost superimposable in these SNAs regardless of postures. Scatter plotting of cardiac SNA over renal SNA during the stepwise changes in CSP was close to the line of identity in 0° supine and 60° upright tilt postures. In addition, upright tilt also shifted the reverse-sigmoidal curve of the CSP-heart rate relationship to a higher heart rate, with increases in the maximal gain and the response range. In conclusion, upright posture caused a resetting of arterial baroreflex control of SNA similarly in renal and cardiac SNAs in anesthetized rabbits.

blood pressure; orthostasis; sympathetic nervous system

SINCE HUMANS ARE UNDER CEASELESS orthostatic stress, the mechanisms to maintain arterial pressure (AP) against gravitational fluid shift are greatly important. During standing, a gravitational fluid shift directed toward the lower part of the body (such as the abdominal vascular bed and lower limbs) will cause severe postural hypotension if not counteracted by compensatory mechanisms (15). Arterial baroreflexes have been considered to be the major compensatory mechanism (1, 13, 15), since denervation of baroreceptor afferents causes profound postural hypotension (16). In addition, we (8) recently reported that upright tilt resets baroreflex control of sympathetic nerve activity (SNA) to higher SNA. The resetting doubles SNA, compensates for the reduced pressor responses of cardiovascular organs to SNA during gravitational stress, and contributes to prevent postural hypotension. However, since the study recorded only renal SNA, it remains unknown whether upright tilt resets arterial baroreflex control of SNA innervating cardiovascular organs (i.e., the heart) other than the kidney. Since cardiac SNA has a critical role in circulation, baroreflex control of cardiac SNA during orthostatic stress is of importance.

Accordingly, in the present study, we tested the hypothesis that upright tilt causes a parallel resetting of arterial baroreflex control of renal and cardiac SNAs in anesthetized rabbits. Since total baroreflex is a closed-loop negative feedback system that senses baroreceptor pressure and controls AP, and since the baroreflex control of SNA (from baroreceptor pressure input to SNA) is a subsystem of the total baroreflex system, it is difficult to isolate the baroreflex control of SNA from the total system in the baroreflex closed-loop condition (16). Therefore, we opened the baroreflex feedback loop by vascularly isolating the carotid sinus region and loaded artificial stepwise intracarotid sinus pressure (CSP) in anesthetized rabbits. By recording renal and cardiac SNAs simultaneously, we investigated static characteristics of baroreflex control of these SNAs (CSP-SNA relationship) in 0° and 60° upright tilt postures.

METHODS

Animals, preparation, and measurements. Japanese White rabbits weighing 2.4–3.3 kg were used. Animals were cared for in strict accordance with the "Guiding Principles for the Care and Use of Animals in the Field of Physiological Science" approved by the Physiological Society of Japan.

Animals (n = 8) were initially anesthetized by intravenous injection (2 ml/kg) of a mixture of urethane (250 mg/ml) and α-chloralose (40 mg/ml). Anesthesia was maintained by continuously infusing the anesthetics at a rate of 0.33 $ml \cdot kg^{-1} \cdot h^{-1}$ using a syringe pump (CFV-3200; Nihon Kohden, Tokyo, Japan). The rabbits were mechanically ventilated with oxygen-enriched room air. Bilateral carotid sinuses were isolated vascularly from the systemic circulation by ligating the internal and external carotid arteries and other small branches originating from the carotid sinus regions. The isolated carotid sinuses were filled with warmed physiological saline, preequilibrated with atmospheric air, through catheters inserted via the common carotid arteries. The intracarotid sinus pressure (CSP) was controlled by a servo-controlled piston pump (model ET-126A; Labworks, Costa Mesa, CA). Bilateral vagal and aortic depressor nerves were sectioned in the middle of the neck region to eliminate reflexes from the cardiopulmonary region and the aortic arch. The systemic AP was measured using a high-fidelity pressure transducer (Millar Instruments, Houston, TX) inserted retrograde from the right common carotid artery below the isolated carotid sinus region. Heart rate (HR) was measured with a cardiotachometer (model N4778; San-ei, Tokyo, Japan).

Body temperature was maintained at around 38°C with a heating pad. The left renal sympathetic nerve was exposed retroperitoneally, and the left cardiac sympathetic nerve was exposed through a middle thoracotomy. A pair of stainless steel wire electrodes (Bioflex wire AS633; Cooner Wire) was hooked onto each of these nerves to record renal and cardiac SNAs. The nerve fibers peripheral to electrodes were ligated securely and crushed to eliminate afferent signals. The nerve

Address for reprint requests and other correspondence: A. Kamiya, Dept. of Cardiovascular Dynamics, National Cardiovascular Centre Research Institute, Suita 565-8565, Japan (e-mail: kamiya@ri.ncvc.go.jp).